The first supernovae and the mass distribution of Population III stars

Martin Mikitas

Lund Observatory
Lund University

2018-EXA136

Degree project of 15 higher education credits
June 2018

Supervisor: Louise Howes

Lund Observatory
Box 43
SE-221 00 Lund
Sweden

Abstract

The properties of the early Milky Way are quite mysterious and some are completely unknown even today. This study is the first one ever to analyze the mass distribution of Population III bulge stars. Using the fitting code STARFIT, we perform an analysis of 65 bulge metal-poor stars obtained by the EMBLA survey to estimate the IMF (initial mass function) of the very first stars that defined our galaxy. We report that the determined majority of stars are low mass in the range of 9.6-15 $M_{\odot}$. Using the whole sample of stars we first perturb all abundances within their own uncertainties 50 times for each star and obtained the best fitting progenitor mass. Thereafter we carry out 50000 iterations of Monte-Carlo simulations on all obtained masses and calculate the mean masses of the progenitors. Upon fitting an IMF we find that this sample is best described by a power-law function with an exponent $\alpha = 1.01$. By removing masses in the mass range of $15 - 30\, M_{\odot}$ we obtain $\alpha = 2.33$, which is almost identical to the one found by Salpeter 1955 and Fraser et al. 2017. The exclusion of these masses is motivated by the fact that an appreciable fraction of the stars in that mass range end their lives by becoming black holes. (Heger and Woosley 2010)

Populärvetenskaplig beskrivning

Att veta hur olika saker i världen kom till hjälper en att släcka den törstiga sömn- förstörande nyfikenheten. Många har ställt sig frågan: hur skapades universum? Någorlunda hela svar har lagts fram (som till exempel teorin om Big Bang), men det finns fortfranade mer att upptäcka. På en relativt mindre skala kan man fråga sig hur skapades Vintergatan? Ännu en fråga delvis svarad med många okända delar. Men detta projekt kommer försöka trassla ut en del av dem okändheter som regerade över Vintergatans tidiga dagar. Big Bang producerade allt väte och helium i universum. När universum svalnat tillräckligt började dessa grundämnen klumpa ihop, vilket i slutändan ledde till formation av de första stjärnorna någonsin, så-kallade första generationens stjärnor. Enligt vår nuvarande förståelse avslutade dessa stjärnor deras korta liv med enorma supernovaexplosioner i vilka nya grundämnen som som kol, kväve, syra, och järn, producerades. Denna nyfödda blandning av grundämnen, inklusive väte, började klumpa ihop sig ännu en gång, och gav liv till nya stjärnor. Eftersom ingenting varar för evigt dog även dessa stjärnor spottande deras bråte över hela universum. Allt eftersom denna cykel återupprepades skapades mer tyngre grundämnen än väte. Grundämnena som finns i solen kommer också ifrån dessa cyklar. Med det sagt så är den kemiska uppsättningen av en stjärna en första indikator av dess ålder. Löst sagt sådesto mindre tunga grundämnen det finns i en stjärna desto längre tillbaka i tiden formades den. Det huvudsakliga grundämnet astronomer använder för att bedöma ålder på en stjärna är järn för att det är enkelt att mäta på tack vare dess stora antal linjer i spektrumet. Med Anglo-Australiska och Magellan Clay teleskopen observerades bulben (centrala delen) av Vintergatan i vilken 65 extremt metal-fattiga stjärnor identifierades och publicerades av Howes et al. 2014, 2015, 2016. Förvånande nog har en av dessa stjärnor 10000 gånger mindre järn i sig än solen, vilket indikerar att den föddes 300 miljoner år efter Big Bang! (För jämförelse har universum existerat i 14,6 miljarder år) Eftersom den har järn i sig alls vet vi att den inte kan vara en första generationens stjärna, men den kan vara en av dess tidigaste avkommor. Den kemiska kompositionen gömmer också det förutnas hemligheter, vilket betyder att genom att analysera spektra kan vi beräkna egenskaperna av föräldrastjärnan (föregångaren) til dessa 65 följdstjärnor, vilket är vad detta projekt kommer att handla om. Detta kommer att göras med ett program som heter STARFIT (Heger & Woosley 2010), vilket skulle passa (kallat fitting på engelska) grundämnens mängd av de 65 bulbstjärnorna till de 17640 teoretiska evolutionära stjärnmodeller och supernovor som kan ha producerat dem. Genom att analysera den bästa passningen kan föregångarens egenskaper bestämmas. Särskilt kommer vi veta föregångarens massa och kvaliteten av passningen. Slutligen kommer dessa egenskaper användas för att bestämma en funktion som beskriver den probabilistiska distributionen av stjärnmassor i den tidiga Vintergatan. Denna studie kommer lägga till ännu en punkt till den kosmiska kanvasen, vilket kommer hjälpa det vetenskapliga samfundet måla en tydligare bild av hur vår Galax såg ut som nyfödd.

Contents

List of Figures

List of Tables

Chapter 1

Introduction

Understanding the early days of the Milky Way puzzles many scientists. Many theories have been put forward, trying to describe the birth and the evolution of the Galaxy but unfortunately they don't fully agree with the observations. These theories build on many assumptions and various unknowns, such as the chemical composition of the early stars and the relative location of their birth. In order to help reduce the number of unknowns, this project is concerned with studying old, metal-poor stars and their chemical composition, which indirectly help us deduce properties of the early Milky way.
The Big Bang produced all the hydrogen and helium in the universe. Once the universe was cool enough these elements started to clump together, which in the end lead to the formation of the first ever stars. These stars ended their short lives with huge supernova explosions in which new elements such as carbon, nitrogen, oxygen and iron were produced. Thereafter, a new generation of stars was born from this new mix, and the cycle of enriching the interstellar medium was repeated, yielding in yet again more and heavier elements. That being said, it's suggestive that the chemical composition of a star contains the information of what came before - insight into the previous generation. It is also considered to be the first indicator of the star's age because ,roughly speaking, the fewer heavier elements there are in the star, the further back in time it was formed. Thus, in this study the stars of very poor metallicities, believing that they are the oldest known stars, that were found in the central part of the Galaxy, were studied because they do porvide insight regarding the very early stages of the Galaxy. In particular the chemical composition of these stars was compared with the output of Pop. III supernovae models, in order to characterize what those Pop. III stars would have looked like. These supernovae models is a result of simulations performed and published by Heger & Woosley 2010. The simulations are packaged together with a matching code which compares the observed chemical composition of star to the database of simulations, and outputs a list of matching candidates that describe the star in question the best.
Similar studies have been performed before, however they have looked at stars that are thought to have been born in a different environment and time from the stars in this study but of similar metallicites. Thus comparison of our results to is essential in order to find any variations. In particular, the predicted masses of found Pop. III stars were used to

recreate a possible IMF (initial mass function) of the first generation stars, and compare with other IMFs (both taken form the halo stars, and those IMFs calculated for the present day Galaxy).
IMF specifies the distribution of stellar masses of a newly formed stellar population in a given volume of space. Usually the IMF is described by a power-law function, with the exponent defining the steepness of the slope and the relative distribution of the stars i.e the number of stars decreases rapidly toward higher masses, and the exponent describes this decrease. The reason IMF is important is because it dictates the fate and the evolution of the galaxy. Studying IMF obtained via different methods helps to us to find possible systematic variations, which in turn help to better understand the physics behind the assembly of the components of the Galaxy.
However the obtained IMF had 3 major drawbacks. The first main one in this study was a relatively small number of stars only 65. The second one was the fact that the simulated supernovae used in the matching procedure were constructed on an irregularly spaced grid, with the main portion of stars lying in the lower mass region. And finally looking at the uncertainties in the supernovae parameters it was apparent that they were non-gaussian. In order to improve our results and obtain a more statistically rigorous IMF, a Monte-Carlo simulation of 50000 was performed.

Chapter 2

Background

2.1 Milky Way

2.1.1 Main structure

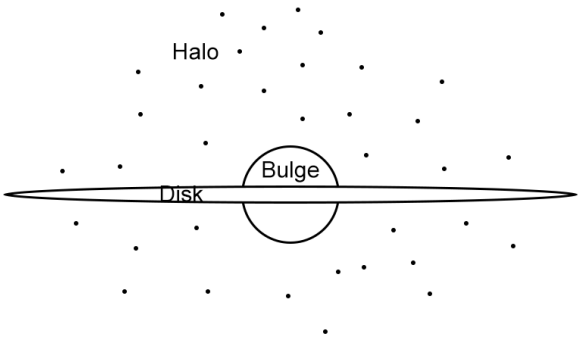

Figure 2.1: Schematic illustration of the Milky Way, showing its main components: Galactic bulge, disk and halo

The Milky Way is a barred spiral galaxy filled with gas, dust and several hundred billion stars with some of them being almost as old as the Universe itself. The latest estimates claim that the universe is 13.799 ± 0.021 billion years old (P.A.R. Ade et al. 2015) while the oldest star is estimated to have formed at least 13.2 billion years ago (Frebel et al. 2007). The size of the Galaxy has been estimated to stretch over more than 100000 light years (Arav et al. 1995).
It's structure could be subdivided into 3 main components: the halo, the disk and finally the bulge which this project will be concerned with. See figure 2.1
The halo is nearly spherical, containing the lowest density of gas as well as stars when compared to the other components of the Galaxy. The stellar component of the halo only contains around 1% of the stellar mass which is between 0.4-0.7 billion solar masses (Bland-Hawthorn and Gerhard 2016). Because there is so little gas in the halo, there is little to

no star formation. The leading theory suggests that it was formed through accretion of surrounding smaller satellite galaxies (Freeman et al. 2002) which could explain the wide range of chemical abundances in halo stars. On the other hand it has been shown that some of the halo stars were formed in the Galactic disk (Abadi, Navarro & Steinmetz 2006) and were ejected into the halo. This means that the opposing theories set limitations on whether the early Milky Way could be studied with the halo stars or not.

The Galactic disk is commonly subdivided into two parts: the thin and the thick disks. The thin disk, being the much larger component, contains around 85% ($= 3.5 \pm 1 \times 10^{10}\, M_{\odot}$) of all the baryonic Galactic mass while the thick disk only has $6 \pm 3 \times 10^{9}\, M_{\odot}$ (Bland-Hawthorn and Gerhard 2016). The currently accepted scale-heights[1] are 300 ± 50 pc and 900 ± 180 pc respectively (Bland-Hawthorn and Gerhard 2016).

Comparing the kinematics it has been established that the stars in the thick disk on average have a radial velocity dispersion of 56.1 ± 3.8 km/s (Pasetto et al. 2012a) while the stars in the thin vary between 30-45 km/s (Pasetto et al. 2012b), with dispersion increasing towards the central region. Another difference is their chemical composition - the stars in the thick disk on average seem to have lower metallicities as well as being older. It has been shown that the thin disk is younger, being on average 6.8-7.4 Gyr old, while the thick is 8.7-9.5 Gyr (Kilic et al. 2017). The thin disk shows a wide age variation and is also responsible for star formation today.

The final component, which this study is concerned with, is the bulge. It is a collection of mostly old stars, but with very varied metallicities. The shape of the bulge has been shown to be resembling a box/peanut (Nataf et al. 2015). The mass is estimated to be around $1.84 \pm 0.07E10\, M_{\odot}$ (which is 1/3 the mass of the disk), the vertical scale-height to be 180 pc and the scale length to be 1.5 ± 0.2 kpc (Wegg & Gerhard 2013). Since our Solar System is located approximately 8.1 kpc away from the center of the Galaxy the study of the bulge proves to be quite difficult because of extinction, which means that the light traveling from the bulge towards us gets absorbed and scattered by the interstellar high density gas along its path, making it diffuclt to study objects there. It is important to note that this project uses data acquired from stars that currently are found in the bulge.

2.1.2 Chemical Abundance and Characterization of stars

The chemical evolution of the Universe started with H, He, Li - elements which were created right after the Big Bang. When the gas was cool enough the primordial cloud consisting of dust, gas and molecules started contracting and forming the very first stars of the universe. As they evolved they produced new elements through nuclear fusion. The new mix was ejected back into the interstellar space (cosmos) via supernovae explosions, refilling the gas reservoir for more star formation. Some of the mass didn't get ejected and ended up in white dwarfs, neutron stars and/or black holes. As the cycle continued, more and more

[1]Scale-height in this context is measured as the distance over which the density of stars decreases by a factor of e

heavy elements were produced. Hence it's plausible to assume that stars which contain fewer heavier elements are by default older stars. For example the first generation of stars to form were produced with the remains of the Big Bang: 75% H and 25% He and small traces of Li (such stars belong to a group of postulated stars called Population III, which have not been observed yet today). Comparing these percentages to the composition of the Sun which is made of 71.54% H, 27.03% He and 1.42% metals (Asplund et al. 2009), it is obvious that it's a much younger star and it was formed after many cycles of chemical enrichment. Stars as our Sun belong to a group called Population I - relatively new stars, with the highest content of metals, primarily found in the galactic disk. Stars that are old and metal-poor belong to a group called Population II and are mainly found in the stellar halo and the bulge.

The chemical composition/abundance of a star contains indirect information regarding the previous generation of stars, called progenitors, that have had time to produce and eject new elements into the interstellar medium. This study will be mostly concerned with such stars.

Spectroscopy is a technique used to study emitted, absorbed and scattered light. By dispersing the light one can infer various properties of that light and the matter it interacted with. For this project spectroscopy is used to determine the chemical composition of old stars, which in turn allows to determine the properties of the molecular cloud that the star was formed from. Going one step further it is possible to determine some of the properties of its progenitor as well as the energy output of the supernova the progenitor ended its life with. (This is explained in more detail in the next section.)

To compare how chemically enriched a particular star is, a logarithmic scale has been devised. It compares a given star's elemental abundance relative to hydrogen to the solar abundance and is measured in the units of [dex]:

$$[X/H] = log_{10}(\frac{N_X}{N_H})_* - log_{10}(\frac{N_X}{N_H})_\odot \tag{2.1}$$

where N_X is the number of atoms of element X per unit of volume. For example [Fe/H]=0 would mean the iron abundance relative to hydrogen of the particular star is the same as that of the Sun. In contrast [Fe/H]=-4 would mean that it's 10000x less iron abundant than the Sun. Note that astronomers who are looking for metal-poor stars use iron as the first identifier because it's easy to measure due to the large number of lines in the spectrum. Metal poor stars can be categorized as following:

Table 2.1: A table that describes nomenclature of some of the Metal-Poor stars. (Beers and Christlieb 2005)

Name	Acronym	[Fe/H]
Solar		∼0
Metal-Poor	MP	<-1.0
Very Metal-Poor	VMP	<-2.0
Extremely Metal-Poor	EMP	<-3.0
Ultra Metal-Poor	UMP	<-4.0
Hyper Metal-Poor	HMP	<-5.0

At the time of writing, the most iron-poor known star is *SMSS J031300.36-670839.3* (Keller et al. 2014), with the latest analysis constraining its metallicity to at least [Fe/H]=-7.52 (Bessell et al. 2015).

2.1.3 Formation of the galaxy and the initial mass function

The understanding of how our Galaxy was formed has been a hot topic for many generations of astronomers. As new technologies emerged, the pool of knowledge increased and changed the way we look at the formation. There are two competing models. The monolithic (Eggen et al. 1962) and the hierarchical (Searle and Zinn 1978). The monolithic model assumes a rapid collapse of gas followed by star formation. This view favors an isolated evolution of a galaxy, where the initial conditions determine all its future properties. The hierarchical model on the other hands assumes that formation of a galaxy is an ongoing process, driven by smaller mergers of stellar groups. Since the introduction of these models many studies have been done in order to rule out the wrong theory. Even though the latter model is favored by cosmologists due to the better theoretical fit with the observations, the monolithic model cannot be excluded because it too describes some of the properties of galaxies that the former doesn't (Kampakoglou, Trotta and Silk 2008). This complication has been addressed by hybridizing both of the models, yielding the best results. (Springel and Hernquist 2003, Benson et al. 1998). By studying the Cosmic Microwave Background radiation (radiation that was left over after the Big Bang) it has been shown that matter in the early universe was not totally smooth, but instead a little bit clumped. (Smoot 1992, 1999). These clumps are thought be the protocores of the very first protogalaxies in the universe, where the first stars were formed. These protogalaxies would later evolve and merge with each other. Collapsing and cooling they would first form a spheroidal galaxy, and then after some time spiral structure would emerge. If however mergers would happen after the collapse then only elliptical galaxies would form. Observational data shows that there are both types of galaxies, which once again suggests that formation of the galaxy is complex. However, whichever method of formation occurred, the first stars formed in the densest areas, which according to galaxy simulations, are likely to correspond to the centres of larges galaxies, like the bulge of the Milky Way (Springel, White and Hernquist 2001, Brooks 2007)

In order to develop a better understanding of the evolution of our Galaxy one can study the distribution of stars in the early Galaxy using the initial mass function (IMF) and then compare the results to the distribution of younger stars. Mass is arguably the most dominant property of the star which consecutively plays the biggest role in defining its radiation spectrum, luminosity and radius. Distribution of stellar masses entering the main-sequence('birth of a star') at one given event in a given volume of space is defined as the initial mass function:

$$F(m) = Am^{-\alpha} \tag{2.2}$$

A being a constant, m being a mass of a star in solar masses and α being the variable describing the steepness of the slope of the function. The first IMF study (Salpeter 1955), examined stars in the solar neighborhood in the range of 0.4-10$M_{\odot}$ and estimated that the Galaxy is well described by a power-law mass function (Eq. 2.2 with an exponent $\alpha = 2.35$, which suggested that majority of the stars have smaller masses, and as mass increases the number of stars decreases rapidly.

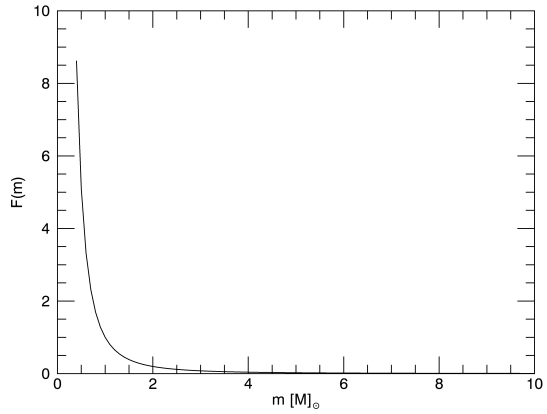

Figure 2.2: Salpeter 1955 initial mass function. Masses in teh range of 0.4 and 10 $M_{\odot}$ are plotted against the exponential mass function $F(m) = Am^{-\alpha}$

This study has been extended towards the lower end of the range $< M_{\odot} = 0.4$ (Scala 1986, Kroupa 2002) and the upper end reaching 150 $M_{\odot}$ (Phillip Massey 1998), finding conflicting results regarding α. Kroupa 2002 study concluded that IMF is extraordinary uniform, being 2.35, meanwhile Geha et al. 2013 study of low-mass stars in the ultra-faint dwarf (UFD) galaxies claims that it should vary dependent on the environment. UFD are least luminous (Martin et al. 2008; Munoz et al. 2010) and most dark-matter dominated (Simon & Geha 2007) galaxies known to date. Their average metallicities are less than typical globular clusters (Kirby et al. 2008).
The most recent study of the metal-poor stars residing in the halo of our galaxy suggests that the early Milky Way is well described by the steepness of the IMF slope of $\alpha = 2.35$ (Fraser et al. 2017), yet again strengthening the claim that IMF is uniform.

2.2 STARFIT

Running the clock backwards to figure out the properties of what came before is not an easy task. The study that took 5 years to complete simulated the evolution of metal-free stars. (Heger and Woosley 2010). The end result was the now readily available online program called STARFIT[2]. As an input it accepts the chemical abundances of an observed star and as an output it lists the properties of 10 best fits of the supernovae that came before, such as the initial mass of the star, supernova energy and internal mixing of elements. The rank of the fit is determined by the χ^2-fit, where the smaller value represents a better fit. The χ^2-test (goodness of a fit) tells you how well the observational data fits the model and is given by:

$$\chi^2 = \sum_{i=1}^{N} \frac{(F_i + O - D_i)^2}{\sigma_i^2} \tag{2.3}$$

Where F_i is the fit value, O is the offset constant, D_i is the observed elemental abundance and σ is the uncertainty. Input metallicity is fitted to 17640 various evolutionary star-models. These models were simulated by taking 120 stars of different masses between 9.6 and 100 solar masses with initial metallicity of zero, which were exploded with 10 different kinetic energies at infinity ranging between 0.3 B and 10 B (B=10^{51}Erg). The location of source of the supernova explosion within the star was varied for energies of 1.2B and 10B. Mixing was artificially simulated by using a moving boxcar average (1D) of width ΔM, n number of times. Thereafter the nucleosynthetic chemical yield was accurately determined. Models assumed that the stars did not rotate and did not undergo mass loss during the evolution.

Comparing these models to a sample of a few metal poor stars, the authors concluded that the program usually finds a good fit, especially for UMP stars. They suggested the reason it's not a perfect fit is due to the limitation of the models: mass range, no rotation, as well as unrealistic mixing (because it's a multidimensional effect whereas the code is only one-dimensional) and the incomplete picture of the physics behind supernova explosions (including asymmetric explosions). Additionally the authors repeatedly stress the fact that the program is intended to find a zero-metallicity progenitor meaning the observational data should be of the second generation 2 stars. Any trace of metal in the abundance of the progenitor would produce inaccurate results.

2.3 Previous studies

The above mentioned program was used in several other studies of observational data which are shortly summarized below.

[2]STARFIT can be found at http://starfit.org

2.3.1 Placco et al. 2015

In a study done by Placco et al. 2015, high resolution spectra of 2 halo UMP stars were presented and together with 20 literature stars were analyzed using STARFIT. It was found that the fitting procedure is highly sensitive to Carbon and Nitrogen abundances. By analyzing a set of literature stars with STARFIT it was determined that the progenitor masses for the UMP stars ([Fe/H] <-4.0) lie in the range of 20.5-23.0 $M_{\odot}$ or 27-28 $M_{\odot}$ and supernova explosion energies between 0.3-0.9 $\times$ 10^{51} erg.

2.3.2 Fraser et al. 2017

In a study done by Fraser et al. 2017, abundances of 53 EMP stars taken from halo stars in the literature were analyzed using STARFIT. Once it showed the quality of the fit was good, an IMF (initial mass function) was fit to a subset of 29 stars ($[\chi^2]$ <3) and it was determined that exponent α=2.35 describes the progenitor IMF the best with M_{max}=87M and M_{min}=8.5M. However due to the limitations of STARFIT it was concluded that the lower mass limit may be even lower. Finally the authors speculate that due to the fact that the exponent is 2.35, which is the same as predicted for the present day Galaxy as was mentioned earlier, maybe the star formation in the early Universe was not too different from what it is today. However considering such a small sample of stars no firm conclusions should be drawn. The metallicites of the metal-poor stars were acquired from published literature. Before running the data through the STARFIT-code, the abundances were randomly perturbed within their uncertainties 30 times per star, which resulted in 65×30 array of masses. Thereafter from that array a random mass was drawn 50000 times per star (as in 50000 times per row) resulting in a new array of 65×50000 masses. For each star(row) the mean mass was calculated and plotted. Finally a cumulative IMF was fit resulting in the above mentioned exponent. A similar procedure was used in this project and thus is described later in the method section in more detail.

2.3.3 Bessell et al. 2015

In a study Bessell et al. 2015 the authors obtained UV spectroscopic data of a halo star SM0313-6708 published by Keller et al. 2014. This star was shown to have no iron abundance at all and an excessive abundance of carbon and magnesium relative to calcium. The high S/N ratio of the UV data allowed the authors to set the iron abundance to be at most [Fe/H]=-7.52, as well as set an upper limits on nitrogen, Fe-elements and some α-elements. By running this star through the STARFIT code they found that the progenitor mass lies in the range of 40-60 $M_{\odot}$, energies 1.5-1.8 B and most likely originated from a single massive Population III progenitor.

2.4 Data used in this project

Within the CDM framework (cold dark matter) it was shown that the oldest stars in the Galaxy reside in the bulge (Springel, White & Hernquist 2001, Brooks et al. 2007). This project uses data which was published in the papers called 'The EMBLA survey' (Howes et al. 2016, Howes et al. 2015) and The Gaia-ESO Survey' (Howes et al. 2014)
In the first paper the bulge was imaged with the SkyMapper telescope. The photometric data which contained a number of stars on the order of 10^7 was reduced down to a smaller subset of potential metal-poor stars.
Thereafter using the Anglo-Australian Telescope with medium resolution (R=10000) spectroscopic data of 14000 stars (subset) was acquired. The calcium triplet was used to determine metallicity very accurately and confirm the metal-poor nature of the candidates found with SkyMapper. Once MDF (metallicity distribution function) was fit, it was found that the average metallicity was [Fe/H]=-1 with a long tail into very metal-poor region [Fe/H] <-3. The stars from the tail were selected as the primary candidates and thus studied with a high resolution spectrograph on the Magellan telescope in order to determine their detailed chemical composition. For now it's still unclear whether or not these stars are just halo stars passing by the bulge, or they are true bulge stars on tight orbits around the center of the Galaxy. If the latter is true, then it could be assumed that they were formed at earlier redshifts (earlier times of the formation of the Galaxy imply older stars). Nevertheless, in the future the orbits will be possibly constrained with the help of the upcoming Gaia kinematic observational dataset. However because these stars are 8 kpcs away and their emitted light is heavily absorbed and scattered by the interstellar dust and gas they appear dim, which will directly increase the uncertainties of the orbits. For the time being a small fraction has been analyzed using proper motion data from the OGLE (Optical Gravitational Lensing Experiment) kinematics catalog. The results proved promising and showed that at least 5 out of 10 stars belong to the bulge, which means potentially these stars formed at redshifts of z >10 (450 millions years after the Big Bang). Putting together all the high resolution data a total of 65 metal-poor stars were observed. The average metallicity of the sample was found to be [Fe/H]=-2.7 as seen in Figure 2.3

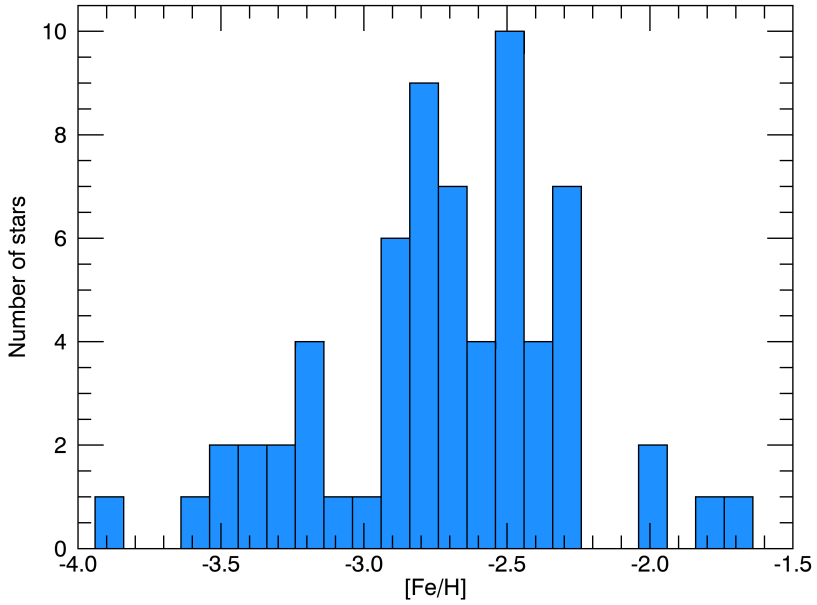

Figure 2.3: Metallicity distribution of the sample

Chapter 3

Method

3.0.1 Evaluation of the STARFIT offline code

Online and offline comparison

Running the online version of STARFIT on each star from the sample would definitely work but in the end would be very limiting and time-consuming making it harder to vary the settings and apply to a batch of stars, thus program code together with its auxiliary files, including the supernova model database `znuc2012`, were downloaded from the official homepage. This database contains 17640 models of the simulated supernovae described in the previous chapter. Once the folder structure was recreated the program was compiled within `IDL 8.4`. Before proceeding with the data analysis it was vital to ensure that the offline version produced the same results as the online one. Using the provided observational data of the star `HE1327-2326` (Anna Frebel 2006), the code was executed using the default[1] recommended settings.

Variation of the defaults options

In order to get a better understanding of the fitting output, default options that are available by the online procedure were varied offline. The simulated models tend over/under produce some elements such as Cr and Zn. To accommodate for this, the option of the *underproduction* can be varied. In the code it is treated as a lower limit and is recommend to be set to Sc and Cu, because these elements can have other nucleosynthetic contributions than modeled. The second option, (*ignore*), allows for the exclusion of elements. By default it is set to Z> 30 (elements heavier than Zn), because the origin of such elements in Population III stars currently is not fully understood. And the final option allows for combination of C, N and O. Theoretically the abundance of these elements should be consistent throughout a star's life because they are being cycled to produced heavier elements. Since it can be difficult to measure nitrogen abundance accurately, one can correct for this by combining C,N and O.

[1] default options: excluding elements Li, Cr, Zn; setting model lower limits to Sc, Cu; using elements up to Z=30; no CNO combination

The upper part of table 3.1 shows that varying the underproduction has a slight effect on the fit and varying the exclusion has no effect on the progenitor mass. The middle section of the same table however shows that combining C, N and O in different ways has a greater impact both on the χ^2 as well as the mass.

Table 3.1: A table of different combinations of the settings for the underproduction (*ud*), the ignore (*ig* and the CNO combination of the code for the star `HE1327-2326`. Followed are the χ^2 and progenitor masses of the first and the second rank of the fit illustrating the effect different settings have on the final results. First the *underproduction* and the *ignore* options are varied, followed by the combination of CNO and then finally with the variation of all.

Settings	$\boldsymbol{\chi^2_{rank\,1}}$	$\boldsymbol{\chi^2_{rank\,2}}$	$\boldsymbol{mass_{rank\,1}}\,[\boldsymbol{M_\odot}]$	$\boldsymbol{mass_{rank\,2}}\,[\boldsymbol{M_\odot}]$
ud: Sc, Cu *ig:* Li,Cr,Zn	4.4	5.6	21.5	27.0
ud: Sc *ig:* Li,Cr,Zn	4.4	5.6	21.5	27.0
ud: Cu *ig:* Li,Cr,Zn	4.4	5.6	21.5	27.0
ud: nothing *ig:* Li,Cr,Zn	4.4	5.6	21.5	27.0
ud: Sc, Cu *ig:*Li,Cr	4.0	5.2	21.5	27.0
ud: Sc, Cu *ig:* Li, Zn	4.0	5.2	21.5	27.0
ud: Sc, Cu *ig:* Cr, Zn	4.0	5.2	21.5	27.0
ud: Sc, Cu *ig:* Zn	3.7	4.8	21.5	27.0
ud: Sc, Cu *ig:* Li	3.7	4.8	21.5	27.0
ud: Sc, Cu *ig:* Cr	3.7	4.8	21.5	27.0
ud: Sc, Cu *ig:* nothing	3.5	4.5	21.5	27.0
ud: nothing *ig:* nothing	3.5	4.5	21.5	27.0
C+N+O	3.1	3.2	11.6	17.4
C+N	2.8	3.0	11.6	17.6
N+O	2.9	3.0	18.5	17.4
C+O	4.7		21.5	27.1
C+N & *ud/ig* nothing	2.5	2.6	11.6	18.1
C+N+O & *ud/ig* nothing	2.7	2.7	18.1	18.5

Reproducing published data

Next step was to reproduce the results that were published by Placco et al. 2015, in their Table 6, in order to further insure the proper function of the code and gain a deeper understanding of its operation before moving on to our own analysis. For this procedure a subset of the stars and their respective metallicities were obtained and compiled from the published reference papers. The results were summarized in table 3.2. The output progenitor mass was used as a matching criteria. The first column of the table, labeled match, shows that for the majority of the stars, the offline version reproduced the published results perfectly, meaning the output progenitor mass was in perfect agreement with published values. However it's important to mention that for two stars the results didn't

match. The output masses and the supernovae models chosen by STARFIT were very different to the ones published by Placco paper. This could possibly be explained by the use of different abundances. Placco et al. 2015 provides a table of abundances used for the fitting procedure, however, only iron, carbon and nitrogen are listed. These values are different compared to the ones published in the original paper. It is important to note that when authors studied how the χ^2 affected the progenitor mass, they determined that for stars `CS 30336-049` and `HE 1424-0241` mass varied drastically for a very small variation of χ^2. Interestingly enough these are the same stars for which we could not reproduce the results perfectly. This means that a small variation in the abundance will result in a very different mass (this topic is discussed in more detail in the the discussion section).

Table 3.2: UMP stars and their abundances used to reproduce the original results published by Placco et al. 2015. The match criteria is fulfilled when the output mass matches the progenitor mass provided in this table. (Note: the abundance subscript b indicates that the abundance has been corrected using the results from Placco et al. 2014b)

Match	**Star**	**[Fe/H]**	**[C/Fe]**	**C log$_\epsilon$**	**N log$_\epsilon$**	**Mass**	**E [B]**	**Original paper**
Yes	G77-61	-4.03	2.49	7.0	6.4	27.0	0.3	Allen et al. 2012
Yes	HE 0057-5959	-4.08	0.86	5.21	5.9	27.0	0.3	Yong et al. 2013a
No	CS 30336-049	-4.03	0.09_b	4.85	4.7	21.5	0.3	Yong et al. 2013a
No	HE 1424-0241	-4.05	0.63	5.01	4.41	21.5	0.3	Yong et al. 2013a
Yes	HE 0057-5959	-4.08	0.86	5.21	5.9	27.0	0.3	Yong et al. 2013a
Yes	HE 2239-5019	-4.15	1.8	<5.98	<6.38	15.0	10	Hansen et al. 2014
Yes	HE 1310-0536	-4.15	2.53_b	6.72	<6.88	10.9	0.3	Hansen et al. 2014
Yes	HE 0233-0343	-4.68	3.32	7.23	<5.95	11.9	0.3	Hansen et al. 2014
Yes	CS 22949-037	-4.38	1.73_b	5.78	5.95	27.0	0.3	Roederer et al. 2014
Yes	SDSS J1029+1729	-4.99	<0.70	<4.20	<3.10	10.6	0.9	Caffau et al. 2011a
Yes	SDSS J1313-0019	-5.00	2.96	6.39	6.29	27.0	0.3	Frebel et al. 2015
Yes	SMSS J0313-6708	<-7.80	>5.39	6.02	<3.63	41.0	1.2	Bessell et al. 2015

3.0.2 Modification of the code and data analysis

Data entry of the 65 stars

Using the provided observational data of the 65 bulge stars obtained from the EMBLA-survey, a respective file was created for each star and formated for the STARFIT input. (See the appendix for the full observational data set.) These files were later placed in the appropriate folder and the first modification of the main code followed.

Mass distribution histograms

The main code was first edited to scan the folder containing the observational data and run the STARFIT procedure once for each star. From each iteration the best fitting supernova model and a respective progenitor mass was saved, resulting in 65 masses. The output

masses were saved and plotted in a histogram (figure 3.1) to determine the overall mass distribution of the sample.

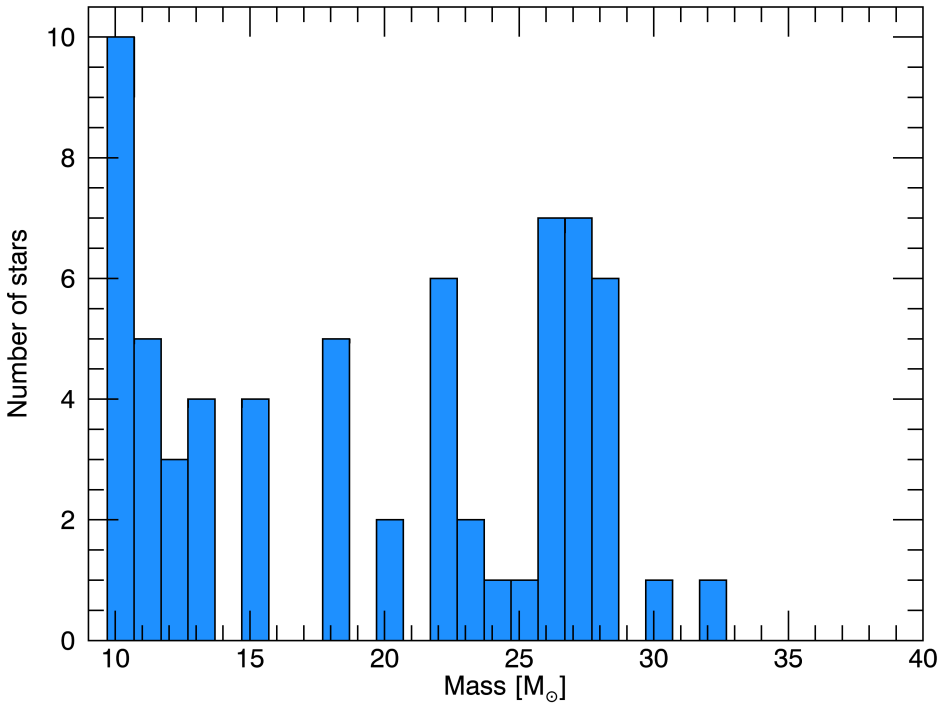

Figure 3.1: Total mass distribution of progenitors obtained after running the STARFIT procedure on the whole sample of 65 bulge stars.

A quick overview of the figure indicates that majority of the stars are in the low-end of mass distribution, around 10 $M_{\odot}$. To smooth out the distribution a histogram with 5 bins were plotted instead which is seen in Figure 3.2.

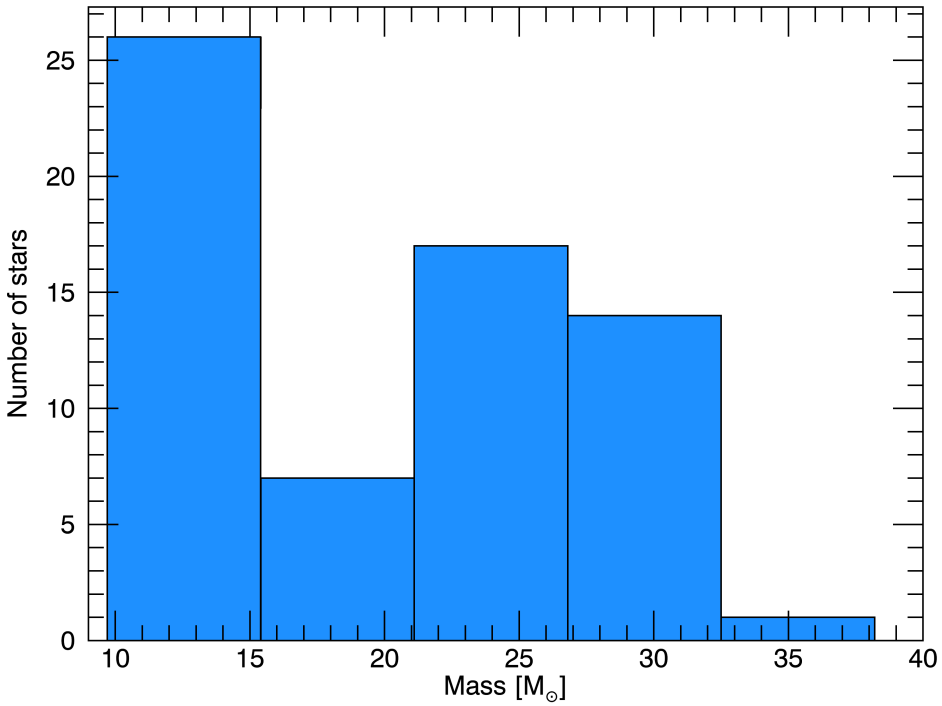

Figure 3.2: Total mass distribution of progenitors obtained after running the STARFIT procedure on the whole sample of 65 bulge stars. A total of five bins have been used to smooth out the gaps that appear due to the discontinuous distribution of simulated masses.

This will be discussed in further detail in the last section.

3.0.3 Perturbation of abundances

Even high resolution spectroscopy contains error. In order to gain a deeper understanding of how the output values depend on the accuracy of the data it was decided to perturb the given values within their own uncertainties. (As was done in Fraser et al. 2017) The code was modified to change the abundance of the element by replacing it with a random value, picked from within the range of possible values from the normal distribution, constrained by the uncertainty. This procedure was repeated 50 times for each star, perturbing every value, resulting in an a two-dimensional array of 50×65 data points.

Distinguishing the results

To have a better overview of the data the results were plotted as a grid of 65 histograms. Each histogram contains results from 50 abundance perturbations. An example of 4 such

histograms is shown in Figure 3.3. The complete table of histograms can be found in the appendix.

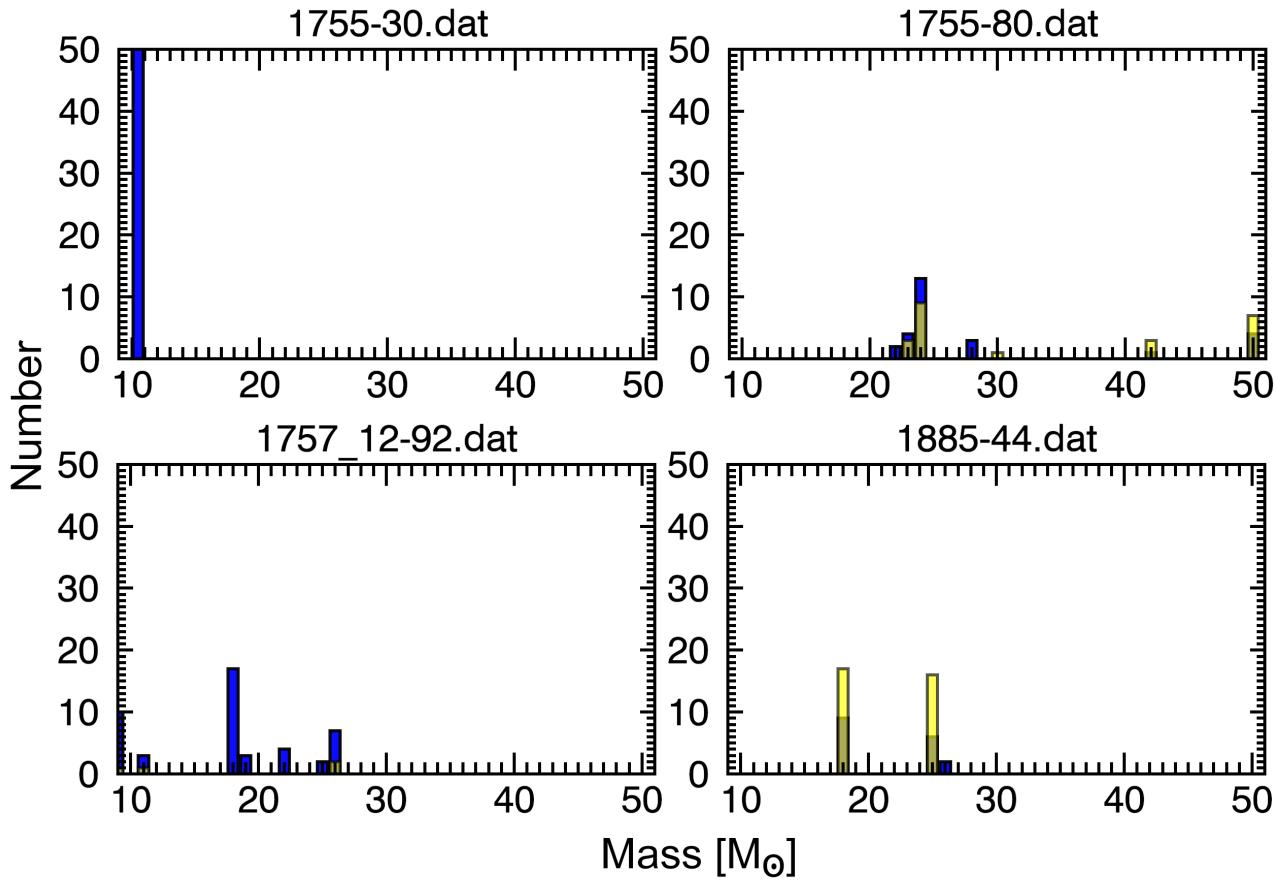

Figure 3.3: An example of four mass distribution histograms for 50 different iterations of random abundance values picked from within normal distribution. Full sample can be found in the appendix.

The output masses with $\chi^2 < 3$ are plotted in blue and $\chi^2 > 3$ in yellow. Since the results of this project are later compared to other studies (such as Fraset et al. 2017 which also uses $\chi^2 = 3$), in order to be consistent, the χ^2 of 3 was chosen as separator. Upon examination of the histograms it was noted that majority of the results are in the former category, which indicates that the data fits the models quite well and that the functionality of the code can be trusted. Looking at the star `1755-30` we see that all 50 perturbations resulted in the progenitor mass of 10 $M_\odot$, however star `1757_12-92` showed a much wider spread, which can be attributed to bigger abundance uncertainties, which directly impacts the value the original abundance was replaced with. Similar spread of masses happens for the stars `1755-80` and `1885-44`, however a noticeable fraction of the results are of lesser quality of the fit ($\chi^2 > 3$). For `1755-80` the majority of masses are around 24 $M_\odot$, and one can see that 'blue' masses around that value seem to be distributed pretty close to

each other, which could potentially mean that the progenitor mass might be lying closer to one value than another, and perturbing the abundance by just a small value, makes STARFIT select a slightly different model (just like rounding off a value up or down). For `1885-44` there is a much smaller spread for both the 'good' and the 'bad' fit, with the code preferring 2 different masses.
In order to verify that there are no trends in the data χ^2-fit was plotted first against [Fe/H] and then against the progenitor mass, shown in figure 3.4 and figure 3.5.

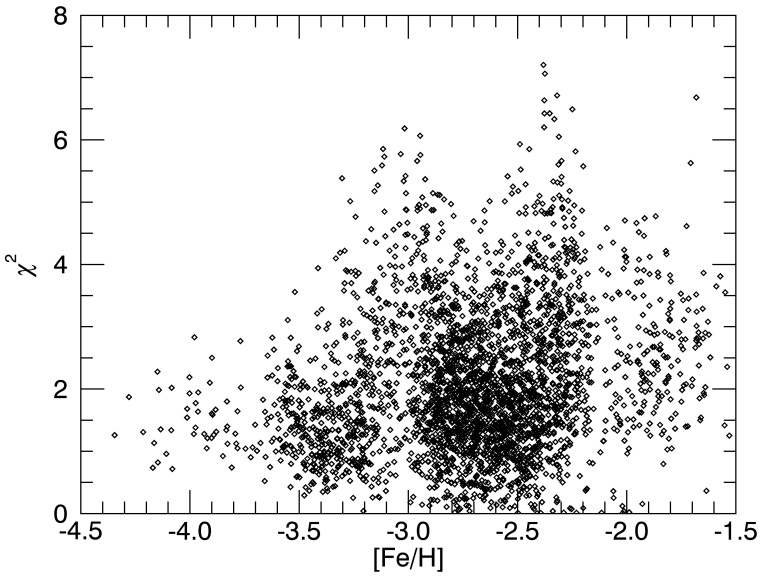

Figure 3.4: χ^2 of the best fit as a function of metallicity for the whole sample of stars shows no trends.

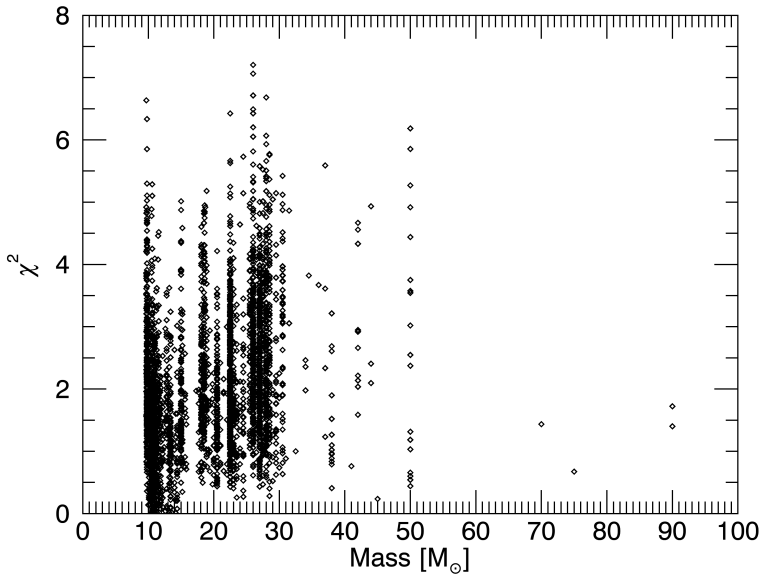

Figure 3.5: χ^2 of the best fit as a function of the progenitor mass for the whole sample of the 65 bulge stars

Figure 3.4 shows no trends. The majority of the perturbed abundances lie in the range of metallicities of -2.5 and -3, just like original values. Evidently we see that for metallicities around [Fe/H]=-4, the variation of χ^2 is greatly reduced, which can depend on the fact that the sample of stars with such low metallicities is also much smaller.
In figure 3.5 grid-like trends are apparent. This plot illustrates that STARFIT models are not continuously distributed. Star-evolution simulations are costly and very time consuming, which lead the authors to choose the model-masses in a step-like fashion.

Monte-Carlo simulation

As mentioned in the introduction a plot similar to Fraser et al. 2017 (figure 4) was needed to be produced in this project. To do so we used double-sampling. The progenitor masses outputted by STARFIT were stored in an array of size 50×65 (50 being the number of masses obtained after each perturbation and 65 is the total number of stars). Thereafter, from this array a random[2] mass was picked 50000 times per each row. Next, each column was sorted in an ascending order and a mean value of each row and the respective errors were calculated with the help of a for-loop. To obtain an upper and a lower error equal to one sigma, the 16th and 84th quantiles were calculated using the function cgPercentiles[3].

[2]Random values were obtained using Carl Salvaggio's 2008 function `RANDOM_SAMPLE`
[3]cgPercentiles is an *IDL Coyote* program available at www.idlcoyote.com/programs

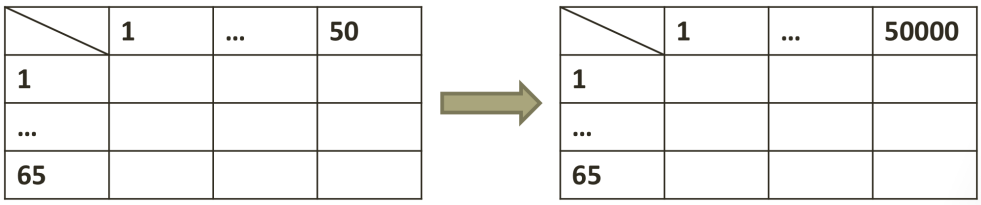

Figure 3.6: Schematic illustration of the double-sampling technique used for the Monte-Carlo simulation. An 50×65 array of masses was sampled to create an array of 50000×65 masses

3.0.4 Curve fitting

Finally, to obtain the IMF function that describes the cumulative data, the power law function (Eq. 2.2) was integrated resulting in:

$$g(x) = B + Cm_{mean}^{-\alpha+1} \tag{3.1}$$

where B and C are constants, and the value of $+1$ in the exponent being a result of integration. This equation was used in the fitting procedure using the least squares curve fitting function `MPFITEXPR`[4] First the fitting was done using with free parameters. Thereafter upon examination it was decided to remove stars in the range of masses between 15-25$M_{\odot}$, in order to see if that would result in a value of α closer to the Salpeter 1955 one of 2.35.

[4]MPFITEXPR documentation can be found at www.physics.wisc.edu/čraigm/idl/fitting.html

Chapter 4

Results and discussion

4.1 Abundance perturbation

4.1.1 Progenitor masses

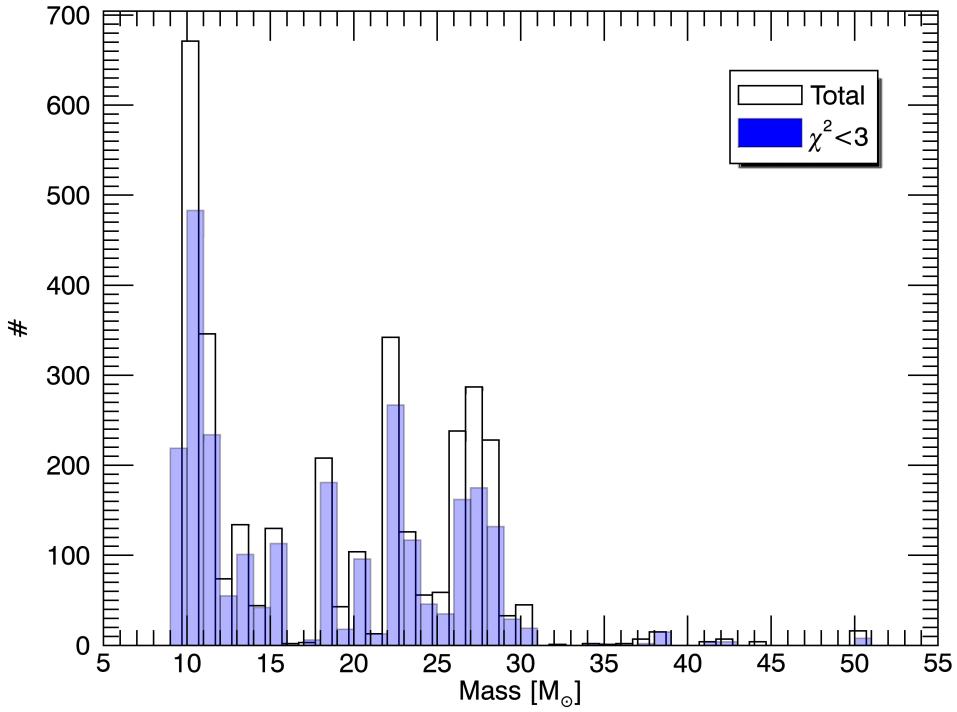

Figure 4.1: A histogram of all output masses obtained after perturbing the abundances within their own uncertainties. The green bars show the total mass distribution and the blue bars show only the $\chi^2 < 3$ results

Figure 4.1 shows a full overview of the mass distribution with 2 clear peaks at 10 $M_\odot$ and $27M_\odot$. Even though they are most pronounced in the total fit, they are clearly dominant in the $\chi^2 < 3$ ('blue-bars') distribution as well. The fact that the majority of the results are of good fit, underlines that the STARFIT results are credible. There is also a potential for a third peak at 23 $M_\odot$, however based on the mass distribution in the range of 15-25 $M_\odot$ it's hard to tell if it's a real peak. The lack of high-mass progenitors in the results can be explained by the fact that the there are no progentiors with masses higher than $35M_\odot$ in the unperturbed results as can be seen in Figure 3.1.

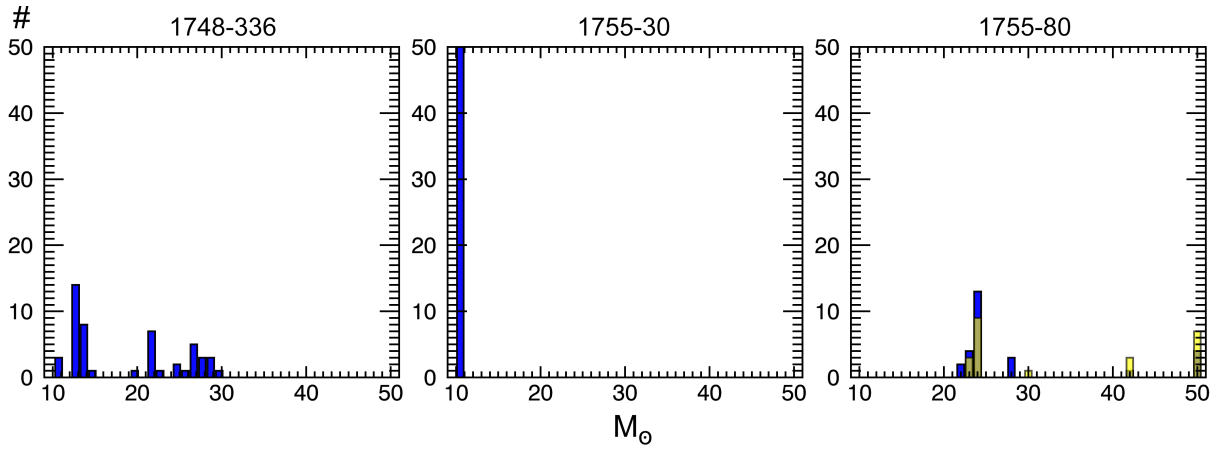

Figure 4.2: Three example-histograms representative of the whole data set which can be found in the appendix. From the left: moderate, good and bad results. The progenitor masses were obtained after perturbing the abundances within their own uncertainties

Perturbing the abundances within their own uncertainties results in three possible outcomes depending on the star. The first case is illustrated in Figure 4.2 star `1755-30` - for all variations of the abundances, for $\chi^2 < 3$ the progenitor masses are always the same. What's different is the mixing and fallback. During a star's lifetime and before the supernova explosion the amount of internal mixing of elements varies. The elements that happen to be closer to the surface are more likely to be ejected into the interstellar medium, and the elements which are closer to the core are more likely to end up in the remnant (such as a black hole, a neutron star or a white dwarf). This means that even though the progenitor mass is the same, the amount of elements that are expelled and produced in the following nucleosynthetic supernova event will vary. Nevertheless, in this example the fitting results are really good, and thus the probability of the progenitor being a first generation star is high. The second representative case is the star `1748-336`. It can be seen that the masses are distributed over a wide range, between 12-42 $M_\odot$, but surprisingly the best fit is still $\chi^2 < 3$. This could mean that even though the uncertainties that affect the abundance perturbation are large, the models chosen by STARFIT are still acceptable, and require further fine-tuning of the code (such as mixing). The final case is the star `1755-80` which doesn't only have a wide spread of masses but also significantly varies in the quality of

the fit (Yellow bars indicate and $\chi^2 > 3$). Just as with the second case, this one requires even more fine-tuning of the models. It's important to note that such a star maybe should be even excluded from the analysis as it could've been created in different conditions than the ones modeled in STARFIT. However the first and the second case show a good fit, and thus giving us confidence in the results. Judging from the Figure A.1, it looks like 17 out of 65 stars belong to the first case, where all or the majority (more than 50%) of the progenitor masses are the same mass. 34 stars belong to the second case (wide range but $\chi^2 < 3$ and the remaining 14 stars belong to the third case $\chi^2 > 3$.

4.1.2 Progenitor mixing and energy output

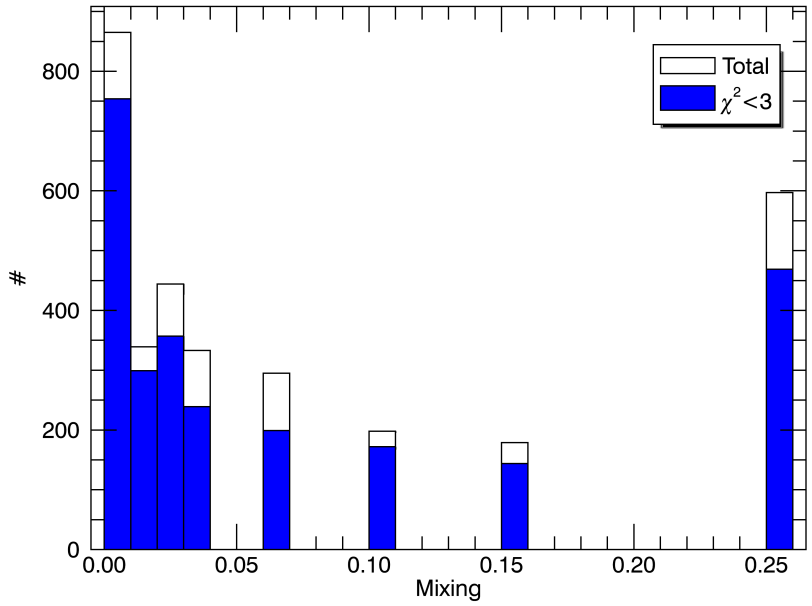

Figure 4.3: A histogram of mixing obtained after abundance perturbations. The white bars show the total sample and the blue bars show results for $\chi^2 < 3$. The x-axis show the fractional mass of the helium core, which was used as the width of the boxcar average in the simulation of the chemical mixing process of the star.

Mixing plays a major role in the nucleosynthetic production. As seen in the previous section for the first-case stars, where all the potential progenitor masses are the same , the mixing varies. It was decided to find the distribution of mixing among the progenitors. Since STARFIT together with masses outputs the respective mixing parameter, the distribution of mixing for all found masses plotted in Figure 4.3. It suggests that mixing of the first

generation stars was low (as was also determined by Heger & Woosley 2010). However it can be seen that there is also another noticeable fraction of stars with mixing of $0.25 M_{He}$.

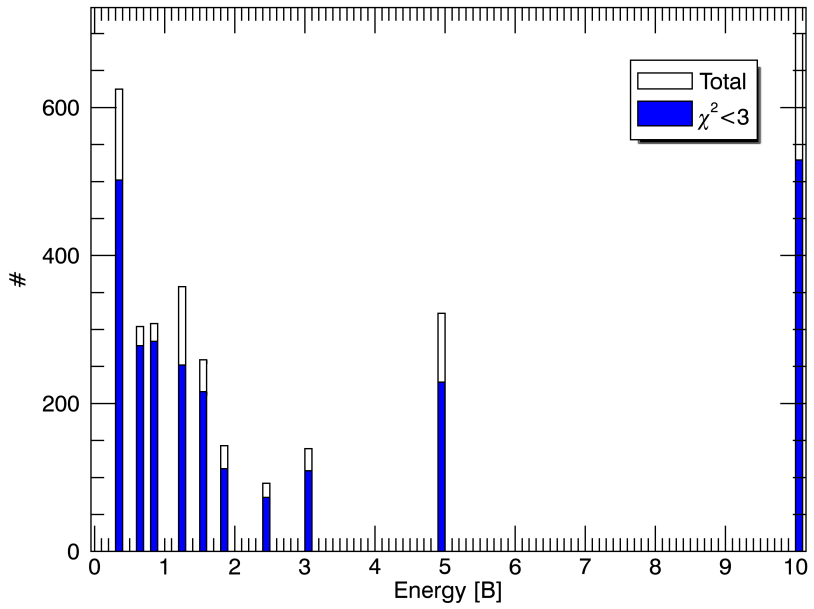

Figure 4.4: A histogram of supernovae energies outputted by STARFIT for each iteration of abundance perturbation. The white bars show the total sample and the blue bars show results for $\chi^2 < 3$. One unit of [B] is equal to 10^{51} erg

Looking at Figure 4.4 we can see that the majority of the supernova explosions are of low energies, with a peak at around 0.3 B. However, there are two more noticeable features - the peaks at 5 B and 10 B which don't have any surrounding distribution. This could be explained by the fact that the authors of STARFIT chose to model lower energy intervals more frequently because their results showed no need for simulations of more energetic explosions. However, looking at our results it's clearly seen that an extended amount of explosions are in the high energy range and require further investigation. Theoretically, there are two types of such high energy supernovae that could describe our results. The first type is a jet-induced hypernova (Tominaga 2009) and the second is a pair-instability supernova. The latter candidate is more unlikely because it requires progenitor masses in the range of 140-250 $M_{\odot}$ (Kassen et al. 2011) and our results show no signs of stars of more than 90 $M_{\odot}$, with an overwhelming majority being much much lower. The study of hypernovae could offer very important insights into how the first generation stars ended their lives and how their supernovae apply to our sample of stars, however it is beyond the scope of this work and we refer the reader to other published literature on this matter.
Finally it's important to note that the stars are distributed in figures 4.3 and 4.4 in a

similar fashion, which requires further analysis.

4.2 IMF results

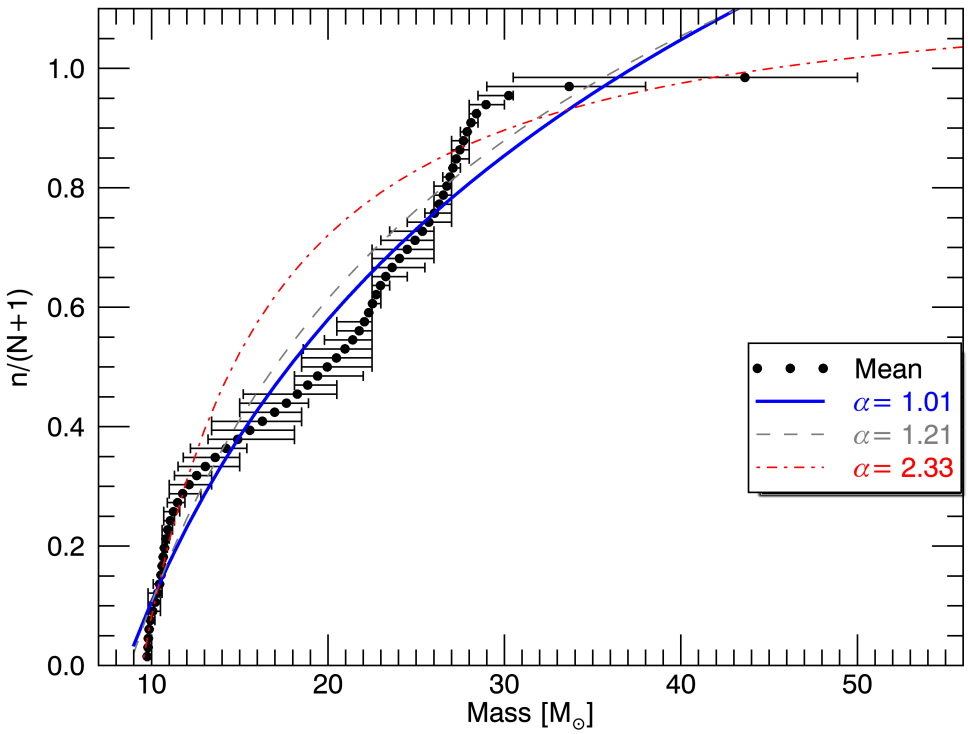

Figure 4.5: IMF fitting to the cumulative distribution of progenitor masses. Black points are the mean masses of the n^{th} star across all 50000 Monte-Carlo iterations. Error bars correspond to 16^{th} and 84^{th} quantiles, which equals to uncertainty of approximately 1σ. Blue curve corresponds to a free-parameter fit, while the red fit excludes masses between $15 - 30\,M_{\odot}$.

Looking at the best fit, indicated by the blue line in figure 4.5, the results could be described by a power-law function with exponent $\alpha = 1.02$ (which is very different to one found by Salpeter et al. 1955 and Fraser et al. 2017: $\alpha = 2.35$) In general the quality of the fit seems to be quite moderate. For a majority of data points the curve lies within the error bars. The best agreement happens at lower masses, which could be explained by the fact that the majority of the progenitor masses output by STARFIT were low mass stars around $10M_{\odot}$ as can be seen in figure 3.2 and 4.1. For greater masses the fit seem to worsen and the IMF is pulled toward a flatter slope. The first major departure is visible in the region of 19-24$M_{\odot}$ and the second one between 27-30$M_{\odot}$. Fraser et al. 2017 also seem to have a similar feature in their results - apparent departure from the best fit in the region of 15-30 $M_{\odot}$. They claim there could be two reasons for that. The first one being the

grid effect of STARFIT (can be seen in figure 3.5) which restricts the masses to certain numbers, distorting the true distribution. However this is very improbable due to the fact that modeled masses are distributed at 0.5 $M_{\odot}$interval, and departure happens within a much greater range. The second, more probable reason, is that a fraction of stars in that region end up their lives in a core collapse resulting in a black hole, meaning the newly created elements are not ejected but rather experience a fallback and don't enrich the next generation of stars. This would mean we wouldnt see the evidence of these stars in the atmospheres of the next generation, and would cause them to be missing in our IMF. Since this feature appears in both, our and Fraser et al. 2017 studies, it was decided to remove a portion of stars, to study the change of the fit. At first the stars in the range of 19-24 $M_{\odot}$ were excluded because the best fit lie well outside their error bars. This however resulted in a small change of the slope resulting in α=1.21, which lead us to extend the stellar mass range to 15-30 $M_{\odot}$. Surprisingly this resulted in α=2.33 which is almost identical to the one found by the above mentioned studies. However this almost 'arbitrary' exclusion should be viewed with caution, since by removing the stars in that mass range we effectively remove 40% of our data points, from our already relatively small sample of 65 bulge stars. The exclusion of the intermediate masses allows for almost a perfect fit a lower masses, however the higher masses are still poorly fit as without the exclusion, which could be an indication that this particular mass distribution is not well described by a power-law. Nevertheless, using the obtained power-law slopes we also calculated the minimum and maximum masses of the stars: For our study, the change of the IMF slope doesn't considerably change the

Table 4.1: Comparison of α determined in this study and Fraser et al. 2017, as well as the minimum and maximum masses they result in.

α	$m_{min}\,[M_{\odot}]$	$m_{max}\,[M_{\odot}]$
1.01	8.9	37
2.33	9.5	45
2.35_{Fraser}	8.5	70-110

max/min masses. The lower mass limit seems to match Fraser et al. 2017 results quite well, though this could be a consequence of the theoretical models used by STARFIT, since the lower mass limit in the simulations was set to $9.6M_{\odot}$, and both of the results are pretty close to this value. More interestingly is the difference in the maximum mass obtained by both studies, which can be attributed by the greatest mean mass produced by the Monte-Carlo simulations. In our study it was 44 $M_{\odot}$ and in Fraser et al. 2017 it was 80 $M_{\odot}$. This had a direct impact on both the IMF and the resulting theoretical maximum mass.

These results can have different interpretations and implications. Assuming that our results are correct and the free parameter α = 1.01 is right, which is hugely different from the values found in studies of today's Milky Way, and that done of Fraser in the Galactic halo, our findings would then support the theory of non-uniform IMF. This argument is further supported by the very different maximum mass determined in the project compared to the

above mentioned studies. All this could mean that the environment in which the stars form has a great impact on the IMF and hence the formation and the evolution of the Galaxy. This in turn could mean that the bulge stars that we have looked at in this study are presumably older and likely to have formed in a different, more dense environment than the halo stars looked by other studies. If the first stars do form in the central region of a galaxy, this could very well mean that the IMF of the early Milky Way was very different to the one that describes the Galaxy today, meaning that the rate of star-formation has changed with time.

On the other hand if the $\alpha = 2.33$ is right then it would then support the theory of a universal IMF, which claims that despite vast differences in the properties of galaxies (such as the age, location, environment) the mass function is always the same. If this were true it would be quite an amazing feature of nature, that wherever you are in the Galaxy (perhaps even in the Universe) the IMF is the same which in term would expand the list of the universal constants (e.g the gravitational constant). This would also mean that the evolution of galaxies is driven by such constant, implying that the rate of star-formation does not change.

However analyzing the previous claims deeper, one can't help but wonder if the models used by STARFIT are not applicable to the bulge stars. The environment in which the bulge stars form must have been very dense, containing a lot of molecular gas, with the first generation stars being distributed in close proximity to each other. If one or multiple supernovae would go off, there would be a big possibility of polluting the protocloud of the stars that we have supposedly analyzed. And as was stated by the authors of STARFIT, the fitting procedure is only valid for a single supernova event, since the models don't take into account chemical yield from multiple sources, nor the presence of even a slight amount of metal, which in the end would alter the simulated evolution of a star. Nevertheless, it's important to note that if greater mass stars are created from a greater bulk of molecular clouds, then the probability that their building blocks came from multiple sources is also higher. Meaning the lower mass stars also have a higher probability to be originated from a single supernova, which could explain why the determined IMF in all cases describes lower mass stars much better than higher.

Chapter 5

Summary and conclusions

In this work, we analyzed a total of 65 metal-poor bulge stars published in the series of papers called 'The EMBLA survey'. We determined their progenitor masses using the freely available online code STARFIT. The code was downloaded for the offline use and its functionality was verified. First we reproduced the results generated by the online version and then the results published in Placco et al. 2015. Upon proper performance, the code was modified to analyze the whole sample of the 65 bulge stars, and produce a mass distribution histogram. Thereafter the abundances were perturbed 50 times within their own uncertainties, by replacing the abundance values with randomly drawn values from within the normal distribution. A grid of plots was produced which showed how the change in the abundance varies the final progenitor mass. This showed that even high resolution data with errors can be produce a whole range of different results, yielding in masses between 10-40 $M_{\odot}$. Two mass peaks were found to be present in the range of 9-12 $M_{\odot}$ and 26-29 $M_{\odot}$ with a potential peak centered at around 23 $M_{\odot}$. Finally a Monte-Carlo simulation was performed by sampling the obtained progenitor masses, resulting in 65 mean masses, to which an IMF was fit. We found that the IMF that describes our results the best has a power-law slope with an exponent $\alpha = 1.01$. Since the quality of the fit worsened in the range of 15-30 $M_{\odot}$, it was decided to exclude these stars, which surprisingly resulted in α=2.33, which is almost identical to the one found by other studies which didn't make any exclusions. We concluded that the early Milky way could very well be described by a different IMF, but cautioned the reader that results could be misleading due to the limitations of the STARFIT simulations.

For the near future we first suggest that since Placco et al. 2015 determined that the STARFIT procedure is highly sensitive to C and N abundance, it would be good to investigate C and N corrections published by Placco et al. 2014 would change the progenitor masses and the IMF associated with them. The paper claims that the obtained photometric spectra of the metal-poor stars is slightly inaccurate due to the surface depletion of carbon due to CN processing on the upper red-giant branch. Second, it would be interesting to study the orbits of the obtained 65 bulge stars using the upcoming release of the Gaia kinematic database to determine if these stars are truly bulge stars and not just passing by.

In the far future it would be good to drastically expand our sample of 65 stars, since we are trying to describe the properties of the galactic bulge which contains billions of stars. It would also be beneficial to add new evolutionary models to STARFIT, which would take into account not only mass loss, the stars outside 9.6-100 $M_{\odot}$ range but also non-artificial mixing (plays a major role in determining the evolutionary model), more frequent energy intervals of supernova explosions at higher energies and finally simulate multiple supernovae events that could have polluted the protoclouds. These changes would help in fine-tuning of the fitting procedure, expand the number of stars that could be analyzed with STARFIT and provide more reliable results, plausibly allowing for a more accurate description of the early Milky Way.

Acknowledgements

I would like to thank Louise M. Howes (Lund University, Department of astrophysics) for support and motivation.

Chapter 6

References

Abadi, M. G., Navarro, J. F., Steinmetz, M., (2006) *Stars beyond galaxies: the origin of extended luminous halos around galaxies* MNRAS, 365, 747-758

Arav,N., K. T. Korista, T. A. Barlow, Begelman (1995) *Radiative acceleration of gas in quasars* Nature 376, 576578

Asplund, M., Grevesse, N., Sauval, A. J., Scott, P. (2009) *The chemical composition of the Sun* ARAA, 47, 481-522

Beers. T., Christlieb, N. (2005) *The Discovery and Analysis of Very Metal-Poor Stars in the Galaxy* ARAA 43, 531-580

Benson,A. J., Cole, S, Frenk, C.S.,Baugh, C. M., Lacey, C. G. (1998), *Hybrid galaxy formation* arXiv:astro-ph/9809171

Bessel, M. S., Collet, R., Keller, S. C., Frebel, A., Heger, A., Casey, A. R., Thomas Masseron, Martin Asplund, Heather Jacobson, Karin Lind, Anna Marino, John Norris, David Yong, Gary Da Costa, Conrad Chan, Zazralt Magic, Brian Schmidt, Tisserand, P. (2015) *Nucleosynthesis in a Primordial Supernova: Carbon and Oxygen Abundances in SMSS J031300.36670839.31* ApJ, 806, L16-L22

Bland-Hawthorn, J., Gerhard, O., (2016) *The Galaxy in Context: Structural, Kinematic and Integrated Properties* ARAA, 54, 529-596

Brooks, A. M., F. Governato (UW), C.M. Booth (Durham), B.Willman (CfA), J.P. Gardner (U.Pittsburgh), J. Wadsley (MacMaster), G. Stinson (UW), T. Quinn (UW) (2007) *The Origin and Evolution of the Mass-Metallicity Relationship for Galaxies: Results from Cosmological N-Body Simulations* ApJ, 655, L17L20

Eggen, O. J.; Lynden-Bell, D.; Sandage, A. R. (1962) *Evidence from the motions of old stars that the Galaxy collapsed.* ApJ, 136, 748

Fraser,1,2 A. R. Casey,2 G. Gilmore,2 A. Heger3,4,5 and C. Chan3, (2017) *The mass distribution of Population III stars* MNRAS, 468, 418-425

Frebel, A., Norbert Christlieb, John E. Norris, Wako Aoki, Martin Asplund (2006) *The Oxygen Abundance of HE 1327-2326* ApJ, 638, L17-L20

Frebel, A., Jarrett L. Johnson, Volker Bromm (2007) *Probing the Formation of the First Low-Mass Stars with Stellar Archaeology* MBRAS, 380, L40-L44

Freeman, K., Bland-Hawthorn, J., (2002) *The New Galaxy: Signatures of Its Formation* ARAA, 40, 487537

Heger, A., Woosley, S. E. (2010) *Nucleosynthesis and Evolution of Massive Metal-free Stars* ApJ, 724, 341-373

Howes, L. M., M. Asplund A. R. Casey S. C. Keller D. Yong G. Gilmore K. Lind C. Worley M. S. Bessell L. Casagrande A. F. Marino D. M. Nataf C. I. Owen G. S. Da Costa B. P. Schmidt P. Tisserand S. Randich S. Feltzing A. Vallenari C. Allende Prieto T. Bensby E. Flaccomio A. J. Korn E. Pancino A. Recio-Blanco R. Smiljanic M. Bergemann M. T. Costado F. Damiani U. Heiter V. Hill A. Hourihane P. Jofr C. Lardo P. de Laverny L. Magrini E. Maiorca T. Masseron L. Morbidelli G. G. Sacco D. Minniti M. Zoccali, (2014) *The Gaia-ESO Survey: the most metal-poor stars in the Galactic bulge* MNRAS, 445, 4241-4246

Howes, L. M., A. R. Casey, M. Asplund, S. C. Keller, D. Yong, D. M. Nataf, R. Poleski, K. Lind, C. Kobayashi, C. I. Owen, M. Ness, M. S. Bessell, G. S. Da Costa, B. P. Schmidt, P. Tisserand, A. Udalski, M. K. Szymaski, I. Soszyski, G. Pietrzyski, K. Ulaczyk, . Wyrzykowski, P. Pietrukowicz, J. Skowron, S. Kozowski, P. Mrz, (2015) *Extremely metal-poor stars from the cosmic dawn in the bulge of the Milky Way* Nature, 527, 484-487

Howes, L. M., Martin Asplund, Stefan C. Keller, Andrew R. Casey, David Yong, Karin Lind, Anna Frebel, Austin Hays, Alan Alves-Brito, Michael S. Bessell, Luca Casagrande, Anna F. Marino, David M. Nataf, Christopher I. Owen, Gary S. Da Costa, Brian P. Schmidt, Patrick Tisserand, (2016) *The EMBLA survey metal-poor stars in the Galactic bulge* MNRAS, 460, 884901

Kampakoglou, M., R. Trotta, J. Silk (2008) *Monolithic or hierarchical star formation? A new statistical analysis* MNRAS, 384, 1414-1426

Kasen, D., S. E. Woosley, and A. Heger, (2011) *Pair Instability Supernovae: Light Curves, Spectra, and Shock Breakout* ApJ 734, 102-115

Keller S. C., M. S. Bessell, A. Frebel, A. R. Casey, M. Asplund, H. R. Jacobson, K. Lind, J. E. Norris, D. Yong, A. Heger, Z. Magic, G. S. Da Costa, B. P. Schmidt, P. Tisserand (2014) *A single low-energy, iron-poor supernova as the source of metals in the star SMSS J031300.36670839.3* Nature, 506, 436-466

Khokhlov, A., Mueller, E., Hoeflich, P. (1993) *Light curves of Type IA supernova models with different explosion mechanisms* AA 270, 223-248

Kilic, M., Jeffrey A. Munn, Hugh C. Harris, Ted von Hippel, James W. Liebert, Kurtis A. Williams, Elizabeth Jeffery, Steven DeGennaro (2017) *The Ages of the Thin Disk, Thick Disk, and the Halo from Nearby White Dwarfs* ApJ, 837, 162-172

Pasetto, S., E.K. Grebel, T. Zwitter, C. Chiosi, G. Bertelli, O. Bienayme, G. Seabroke, J. Bland-Hawthorn, C. Boeche, B.K. Gibson, G. Gilmore, U. Munari, J.F. Navarro, Q. Parker, W. Reid, A. Silviero, M. Steinmetz, (2012) *Thick disk kinematics from RAVE and the solar motion* A&A RAVE, 547, A70

Pasetto, S., E.K. Grebel, T. Zwitter, C. Chiosi, G. Bertelli, O. Bienayme, G. Seabroke, J. Bland-Hawthorn, C. Boeche, B.K. Gibson, G. Gilmore, U. Munari, J.F. Navarro, Q. Parker, W. Reid, A. Silviero, M. Steinmetz, (2012) *Thin disk kinematics from RAVE and the solar motion* A&A RAVE, 547, A71

Placco, V. M., Anna Frebel, Timothy C. Beers, Richard J. Stancliffe, (2014) *Carbon-Enhanced Metal-Poor Star Frequencies in the Galaxy: Corrections for the Effect of Evolutionary Status on Carbon Abundances* ApJ, 797, 21-40

Placco, V. M., Anna Frebel, Young Sun Lee, Heather R. Jacobson, Timothy C. Beers, Jose M. Pena, Conrad Chan, Alexander Heger, (2015) *Metal-Poor Stars Observed with the Magellan Telescope. III. New Extremely and Ultra Metal-Poor Stars from SDSS/SEGUE and Insights on the Formation of Ultra Metal-Poor Stars* ApJ, 809, 136-154

Planck Collaboration: P. A. R. Ade (2015) *Planck 2015 results. XIII. Cosmological parameters* AA, 595, A13 (2016)

Rix, H-W., Bovy, J. (2013) *The Milky Way's Stellar Disk* AAR, 21, 61

Salpeter, E. E., (1955) *The Luminosity Function and Stellar Evolution* ApJ, 121, 161

Searle, L., Zinn, R.,(1978), *Compositions of halo clusters and the formation of the galactic halo* ApJ, 225,

357-379

Smoot, G. F.; Bennett, C. L.; Kogut, A.; Wright, E. L.; Aymon, J.; Boggess, N. W.; Cheng, E. S.; de Amici, G.; Gulkis, S.; Hauser, M. G.; Hinshaw, G.; Jackson, P. D.; Janssen, M.; Kaita, E.; Kelsall, T.; Keegstra, P.; Lineweaver, C.; Loewenstein, K.; Lubin, P.; Mather, J.; Meyer, S. S.; Moseley, S. H.; Murdock, T.; Rokke, L.; Silverberg, R. F.; Tenorio, L.; Weiss, R.; Wilkinson, D. T., (1992) *Structure in the COBE differential microwave radiometer first-year maps* ApJ, 396, L1-L5

Smoot, George F., (1999), *COBE Observations and Results* AIP, 476, 1-10

Springel, V., Hernquist, L., (2003) *Cosmological smoothed particle hydrodynamics simulations: a hybrid multiphase model for star formation* MNRAS, 339, 289-311

Springel, V., Martin White, Lars Hernquist, (2001) *Hydrodynamic Simulations of the Sunyaev-Zeldovich Effect(s)* ApJ, 549, 681-687

Tominaga, N., (2009) *Aspherical Properties of Hydrodynamics and Nucleosynthesis in Jet-induced Supernovae* ApJ, 690, 526536

Wegg, C., Ortwin Gerhard (2013) *Mapping the Three-Dimensional Density of the Galactic Bulge with VVV Red Clump Stars* MNRAS, 435, 1874-1887

Artist's illustration of the Milky Way (2008) *Pearson Education, Inc* Pearson Addison-Wesley

Appendix A

Mass distribution histograms

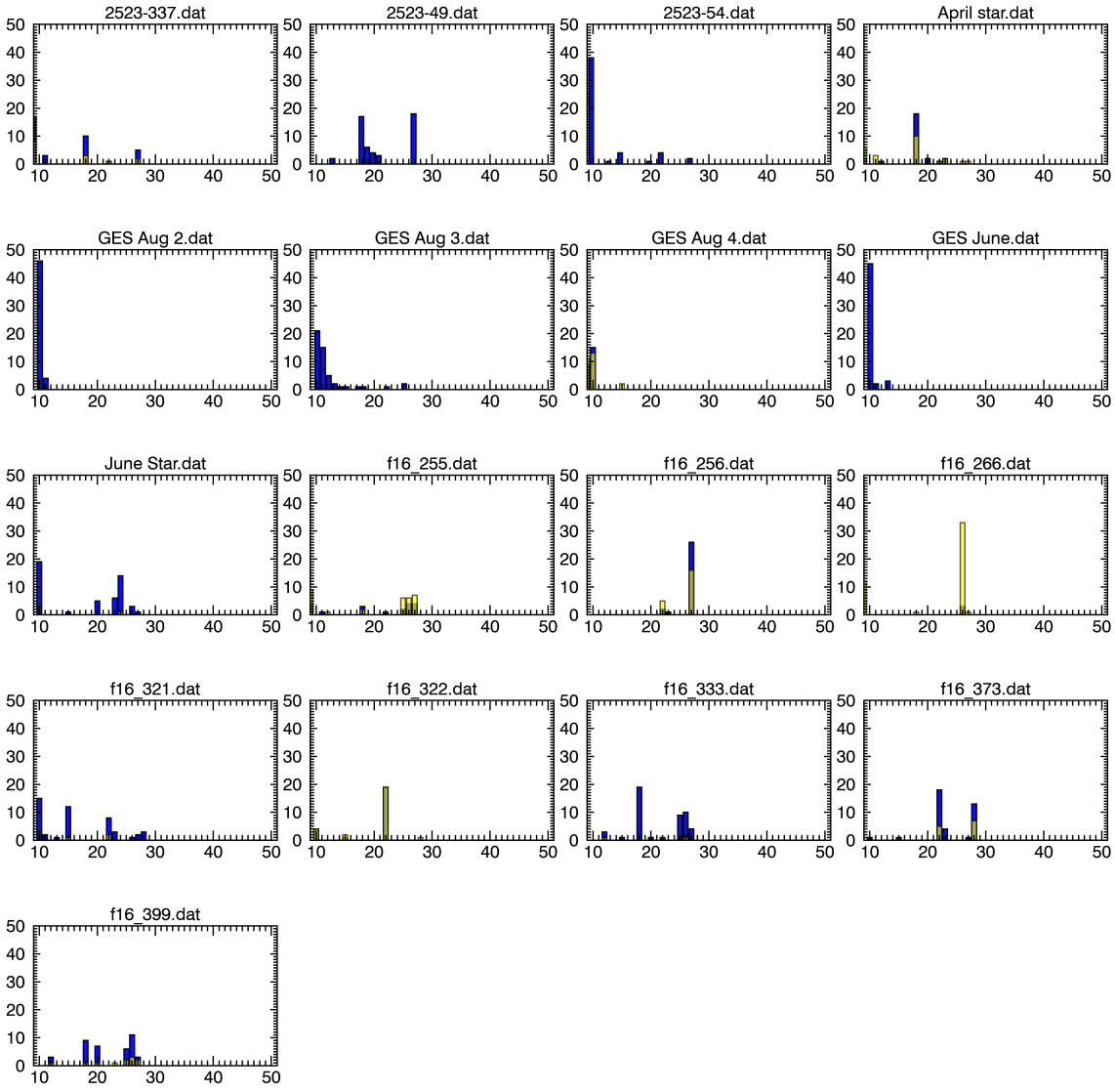

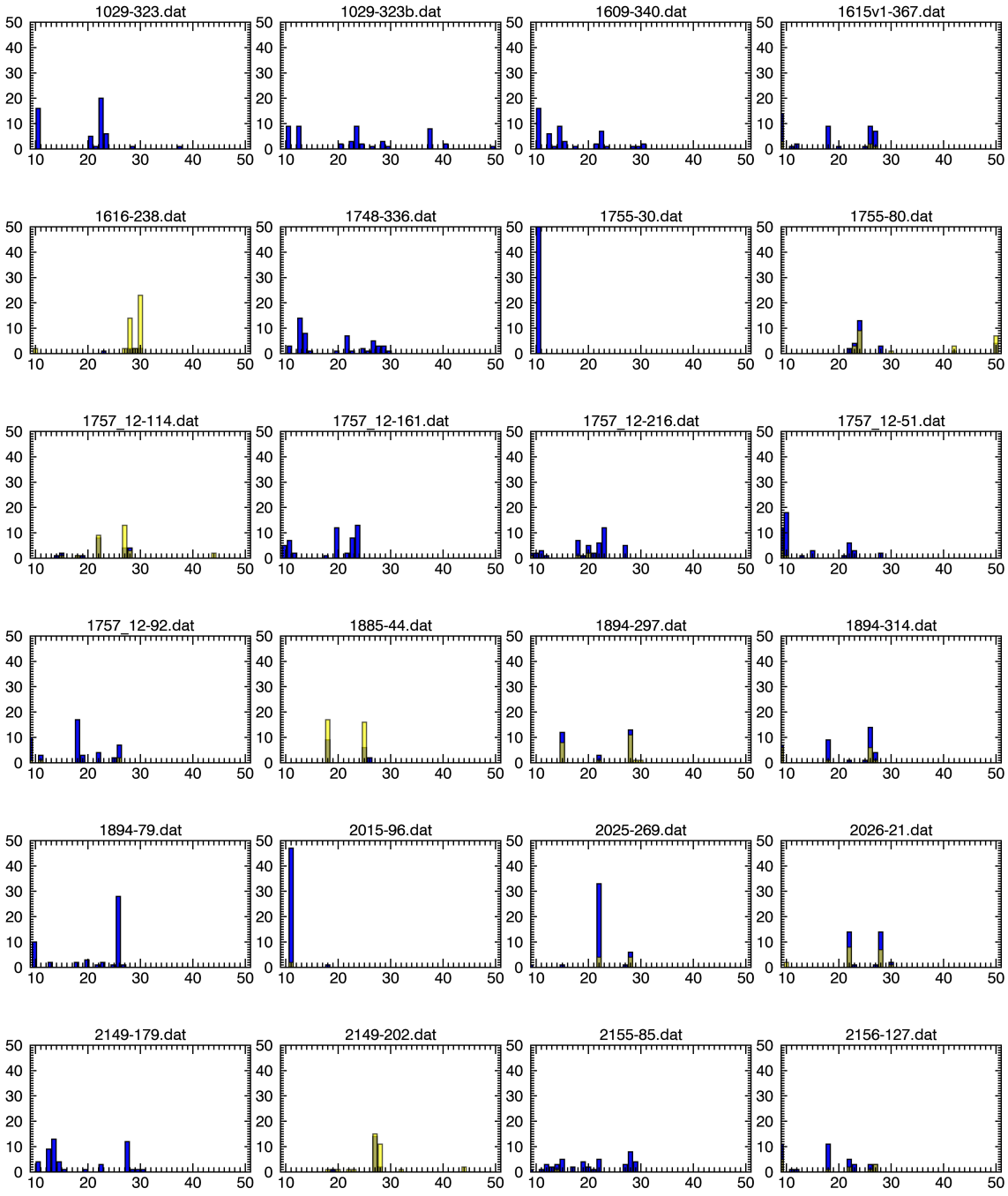
1029-323.dat
1029-323b.dat
1609-340.dat
1615v1-367.dat
1616-238.dat
1748-336.dat
1755-30.dat
1755-80.dat
1757_12-114.dat
1757_12-161.dat
1757_12-216.dat
1757_12-51.dat
1757_12-92.dat
1885-44.dat
1894-297.dat
1894-314.dat
1894-79.dat
2015-96.dat
2025-269.dat
2026-21.dat
2149-179.dat
2149-202.dat
2155-85.dat
2156-127.dat

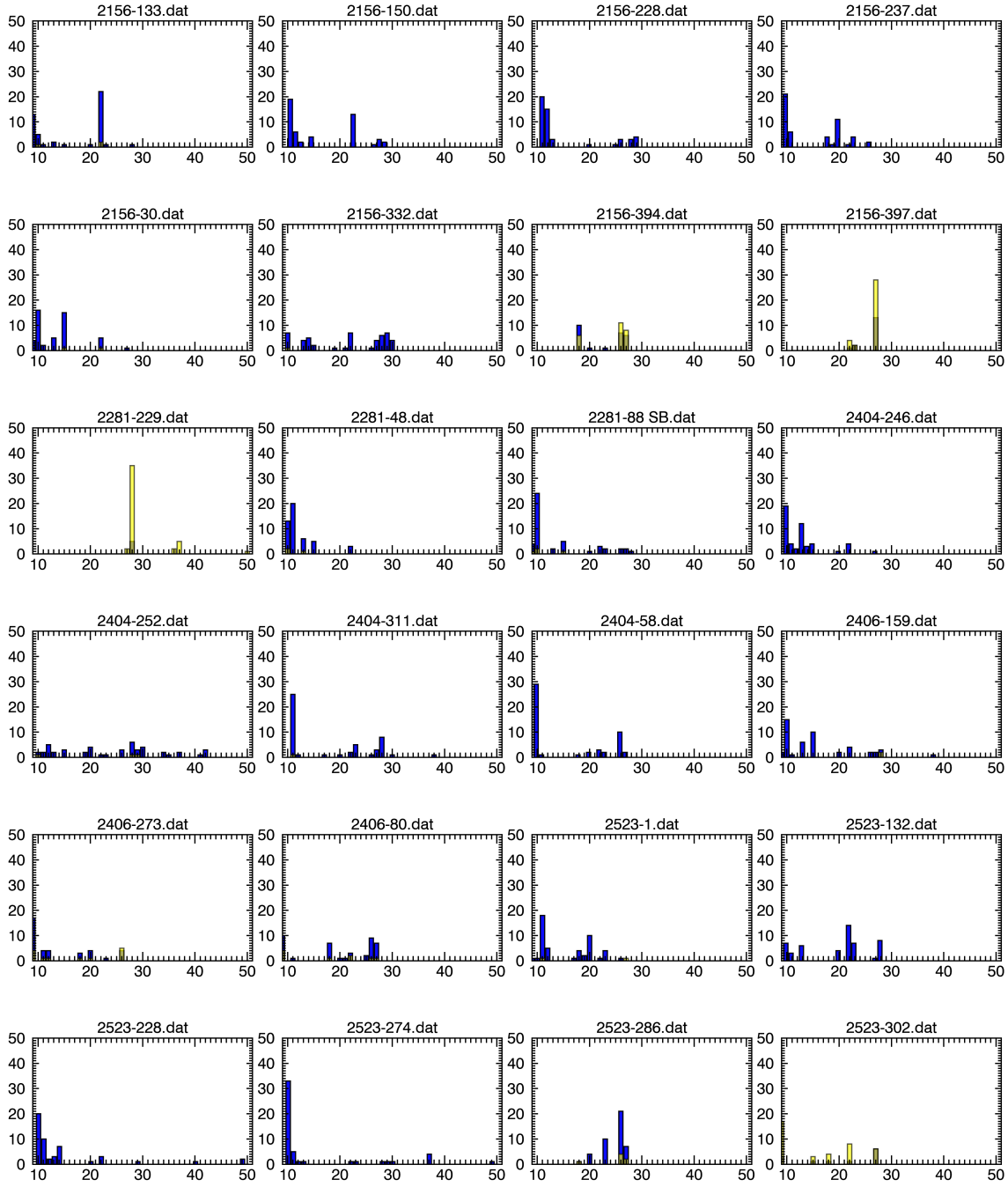

Figure A.1: Mass distribution of the 65 halo stars, where each subplot represents 50 different abundance perturbations. Blue bars are values for $\chi^2 < 3$ and yellow bars for $\chi^2 > 3$.

Appendix B

CODE

```
PRO wrapper ; data_set, stardb, underprod, ignore
choice=0s ;asks the user to either run from scratch or used the presaved variables
READ, choice, PROMPT =’run from scratch press 1. Presaved variables press 2: ’
SWITCH choice OF

;*****************CASE 1 (run from scratch)*****************
1: BEGIN
COMMON SHARE1, shareMASS, shareCHI, shareFE  ;calls common block to get rank 1 fit
try= 0s ;number of loops
READ, try, PROMPT = ’Enter # of cycles: ’
pathfile = FILE_SEARCH(’/Users/Admin/University/Lund/thesis/STARFIT/the65/65stars/*.dat’, /FOLD_CASE) ;tells idl where to look for files
starcount=N_ELEMENTS(pathfile) ;counts number of files in the folder
arrayM = FLTARR(try, starcount) ; creates an array into which progenitor mass will be saved
arrayCHI = FLTARR(try, starcount) ;array fro CHI^2
arrayFE = FLTARR(try, starcount); create an array of FE= abundances
CD, ’/Users/Admin/University/Lund/thesis/STARFIT/the65/65stars’ ;tells the code where to find files
starnames = findfile() ;creates an array of strings, of star names

FOR j=1, starcount DO BEGIN
  FOR i = 1, try DO BEGIN
  starfit, $
     data_set=pathfile[j-1],$
     stardb = ’/Users/Admin/University/Lund/thesis/STARFIT/model_dbs/znuc2012.S4.star.el.y.stardb’, $
     Underprod=[’Sc’, ’Cu’],$
     Ignore=[’Li’, ’Cr’, ’Zn’]
      ;COMBINE=’C+N+O’ $
     arrayM[i-1, j-1]=shareMASS ;grab mass from common block
     arrayCHI[i-1, j-1]=shareCHI   ;grab CHI^2 from common blockl
     arrayFE[i-1, j-1]=shareFE ;grab FE from load_obs_data common block
  ENDFOR
ENDFOR

SAVE, /VARIABLES, FILENAME = ’/Users/Admin/University/Lund/thesis/STARFIT/the65/saved_variables/starfitVars.sav’
END
;
;************ SECOND CASE *************
;
2: BEGIN

RESTORE, FILENAME = ’/Users/Admin/University/Lund/thesis/STARFIT/the65/saved_variables/starfitVars.sav’
iter= 0L ; number of iterations
READ, iter, PROMPT= ’Enter # of iterations fo IMF procedure: ’
;;@@@@@@@@@@@@@@@@@@@@@@@@@@@@@@@@@@@@@@
;;@@@@@@@@@@  P  L  O  T S @@@@@@@@@@@
;;@@@@@@@@@@@@@@@@@@@@@@@@@@@@@@@@@@@@@@
;;===================================
;;--------Full data HISTOGRAM---------
;;
;PRINT, arrayM, arrayCHI, arrayFE
;myWindow = WINDOW(WINDOW_TITLE=’MULTIPLE BARPLOTS’)
;  FOR i=0, starcount-1 DO BEGIN
;    hist=HISTOGRAM(arrayM[0:(try-1), i], location=hlocs)
;    brplt1=barplot(hlocs, hist, title=starnames(i), LAYOUT=[10,7,i+1], XRANGE = [5, 51], XTICKNAME=’’, XTICKINTERVAL=10 ,YTICKINTERVAL=5, YRANGE=[0,30], FONT_NAME=’Times
;    ;;brplt1=barplot(hlocs, hist, title=starnames(i), LAYOUT=[4,17,i+1], XRANGE = [5, 51], YRANGE=[0,30], /current)
;  ENDFOR
;
;;--------Full data CUMULATIVE HISTOGRAM-------
;     hist=HISTOGRAM(arrayM[0, 0:(starcount-1)],locations=hlocs) ;
;     histC = total(hist, /cumulative, /preserve_type)
;     plt1= PLOT( hlocs, histC, TITLE=’Cumulative mass fcn’, XTITLE=’Mass [SolarM]’, YTITLE=’density’, xrange=[9,MAX(arrayM)+5], yrange=[0, MAX(histC)+5], /STAIRSTEP)
;;============================================
;;-------HISTOGRAM with with [FE/H] <3 or >3-----
```

```
;arrayMLT3= arrayM * (arrayCHI LT 3) ; creates an array where all entries of CHI^2 GE 3, are set to 0
;arrayMGE3= arrayM * (arrayCHI GE 3) ; creates mass array for CHI^2 GE 3
;myWindow = WINDOW(WINDOW_TITLE='MULTIPLE BARPLOTS with <3 diff')
;  FOR i=0, starcount-1 DO BEGIN
;    histMLT3=HISTOGRAM(arrayMLT3[0:(try-1), i], location=hlocs)
;    brpltMLT3=barplot(hlocs, histMLT3, TITLE='!C'+starnames(i), LAYOUT=[6,11,i+1], MARGIN=[0.1,0.19,0.02,0.19],XRANGE = [5, 51], XTICKINTERVAL=10 ,YTICKINTERVAL=10, YRAN
;    histMGE3=HISTOGRAM(arrayMGE3[0:(try-1), i], location=hlocs)
;    brpltMGE3=barplot(hlocs, histMGE3, LAYOUT=[6,11,i+1], XRANGE = [5, 51], XTICKINTERVAL=10 ,YTICKINTERVAL=10, YRANGE=[0,30], FILL_COLOR='yellow',  FONT_SIZE=10.5 , /OV
;  ENDFOR

;
;;=========================================
;;----------MASS vs CHI scatter plot------------
;   FOR i=0, try-1 DO BEGIN
;     scat2=SCATTERPLOT(arrayM[i, 0:*], arrayCHI[i, 0:*], /OVERPLOT, $
;            XTITLE='Mass [$M_{\odot}$]', $
;            YTITLE='$\chi^{2}$', SYM_SIZE=0.5, FONT_SIZE=15, XTICKINTERVAL=10)
;   ENDFOR
;
;=========================================
;;----------[Fe/H] vs CHI scatter plot --------
;   FOR i=0, try-1 DO BEGIN
;     scat3=SCATTERPLOT(arrayFE[i, 0:*], arrayCHI[i, 0:*], /OVERPLOT, $
;       XTITLE='[Fe/H]', $
;       YTITLE='$\chi^{2}$', SYM_SIZE=0.5, FONT_SIZE=15)
;   ENDFOR
;------------

;;=========================================
;;----------RANDOM SAMPLING---------------------------------
;;----------STEP 1: create #random ITERATIONS/row array--------
!PATH = Expand_Path('+~/Users/Admin/University/Lund/thesis/STARFIT/coyote/') + ':' + !PATH ;expand path to get Coyote percentile pro

array50K = FLTARR(iter, starcount)
FOR i=0, iter-1 DO BEGIN  ;iteration count

    FOR j=0, starcount-1 DO BEGIN ;
        rw = arrayM[0:*, j] ;extracts a row from arrayM
        array50k[i,j] = RANDOM_SAMPLE(seed, rw, 1) ;draw a RANDOMU number  from a row and put into 50k array
    ENDFOR

ENDFOR
;;---------STEP 2: SORT all the columns-------------
    ;;print,  'rand: ', array50k
FOR i=0, iter-1 DO BEGIN
    g=TRANSPOSE((array50k[i,0:*])) ;extracts the column from the array and transposes
    g=g[sort(g)] ;sorts the row
    g=TRANSPOSE(g) ;transposes it back
    array50k[i,0:*]=g
ENDFOR
;;---------FIND MEAN per ROW and Percentile---------------
meanM=FLTARR(starcount) ;define a flat array to save each mean value for the row
percentile=FLTARR(2,starcount) ; define a flat array to save percentiles in each column which will give us 1 sigma error

FOR i = 0, starcount-1 DO BEGIN
   meanM(i)=mean(array50k[0:*, i])
   percentile(0:*, i) = cgPercentiles(array50k[0:*,i], Percentiles=[0.16, 0.84])

ENDFOR
print, 'means of each rows are: ', transpose(meanM)
;;starorder=INDGEN(starcount, START=1)
starorderCml = FINDGEN(starcount, START=1)/(starcount+1) ;cumulative starorder for Y-axis i/(n+1)
IMFweights = REPLICATE(1.0, starcount)
;;IMFweights[24:45] = REPLICATE(0.0, 22)
;;IMFweights[63:64] = REPLICATE(0.5, 2)
start=[1.d,-0.7,2.35]
expr='imffn2(X, P)'
pi = replicate({fixed:0, limited:[0,0], limits:[0.D,0.D]},3)
pi(0).fixed=0
;;start(0)=1
;;pi(0).limited(0) = 1
;;pi(1).limits(1) = 1
result = MPFITEXPR(expr,meanm,starorderCml,IMFweights,start,WEIGHTS=IMFweights)
;print, result
;----fit with exclusion of some data points-----
IMFweights[20:49] = REPLICATE(0.0, 30)
result2 = MPFITEXPR(expr,meanm,starorderCml,IMFweights,start,WEIGHTS=IMFweights)

IMFweights = REPLICATE(1.0, starcount) ;reset weights
IMFweights[30:44] = REPLICATE(0.0, 15)
result3 = MPFITEXPR(expr,meanm,starorderCml,IMFweights,start,WEIGHTS=IMFweights)

;---------create data points using the formula for plotting------
IMFfitData=imffn2(meanM, result) ;original result
flatX=INDGEN(400,3, START=9)
IMFfitDATA2=imffn2(flatX, result); fitted result
IMFfitData3=imffn2(flatX, result2); fitted without certain points
IMFfitData4=imffn2(flatX, result3); fitted without certain points
```

```
xerr=FLTARR(2, starcount) ;create a flat array to hold errors for plotting
xerr[0,0:*]=meanM-percentile[0,0:*] ;0th coloumn lower errors
xerr[1,0:*]=percentile[1,0:*]-meanM ;1st coloumn upper errors
yerr=FLTARR(starcount) ;create a flat array in order not to plot YerrorBARS
errplt1=ERRORPLOT(meanM, starorderCml, xerr, yerr, SYMBOL='o', SYM_FILLED=1, SYM_SIZE=0.6, ERRORBAR_CAPSIZE=0.09, XTITLE='Mass [$M_\odot$]', YTITLE='n/(N+1)', YRANGE=[0,1

;IMFstring1=string(result[0],FORMAT='(I5.2)')+string(result[1], FORMAT='(I5.2)')+'^('+string(result[2], FORMAT='(F5.2)')+'+1)'
IMFstring1='   $\alpha$='+string(result[2], FORMAT='(F5.2)')
imfpltFIT2=PLOT(flatX, IMFfitData2, LINESTYLE='-', COLOR='blue', NAME=IMFstring1, THICK=2, /OVERPLOT)

IMFstring2='   $\alpha$='+string(result2[2], FORMAT='(F5.2)')
imfpltFIT3=PLOT(flatX, IMFfitData3, LINESTYLE='-.', COLOR='red', NAME=IMFstring2, /OVERPLOT)

IMFstring3='   $\alpha$='+string(result3[2], FORMAT='(F5.2)')
imfpltFIT4=PLOT(flatX, IMFfitData4, LINESTYLE='--', COLOR=125, NAME=IMFstring3, /OVERPLOT)

leg= LEGEND(TARGET=[errplt1,imfpltFIT2, imfpltFIT4,imfpltFIT3], POSITION=[0.92,0.50], /AUTO_TEXT_COLOR)

;MassMAX=(0.01/(-1*result[1]))^(1/(-1*result[2]+1))
MassMax= ((1-result[0])/result[1])^(-1*result[2]+1)
print, MassMAX

END

ENDSWITCH
```